Master's Thesis

# Statistical Characterization of User Effects on MIMO Terminal Antennas

Hayder Al-Zubaidi
Baydai Abdulameer

Department of Electrical and Information Technology,
Faculty of Engineering, LTH, Lund University, March 2014.

Master of Science Thesis

# Statistical Characterization of User Effects on MIMO Terminal Antennas

By

Hayder Al-Zubaidi and Baydai Abdulameer

Department of Electrical and Information Technology
Faculty of Engineering, LTH, Lund University
SE-221 00 Lund, Sweden

# Abstract

In recent years, there has been an increased interest in the communications sector to enhance system performance by achieving higher data rates. This challenge is addressed by MIMO (Multiple-Input Multiple-Output) technology which has become a requirement in recent communication standards such as LTE (Long Term Evolution), HSPA (High-Speed Packet Access) and IEEE 802.11n (WiFi). On the other hand, the aesthetic appeal of small and thin devices such as mobile phones has been one of the primary factors for consumers in deciding their choice of communication devices. Incorporating MIMO technology in communication devices to achieve better performance in harmony with aesthetic design is one of the fundamental challenges for communication engineers. For instance, fitting multiple antennas in a small mobile device is challenging due to the size limitation of current communication devices. Standard requirements dictate that MIMO devices should comprise at least two mobile terminal antennas that cover all communication bands, and these antennas should have high efficiency and low correlation to provide good MIMO performance. Moreover, users have a great influence on antenna performance and therefore user effects must be taken into consideration during the antenna design process in order to maximize the achievable data rates. The main aim of this thesis project is to build a statistically relevant database for the influence that users have on different terminal antennas, and to scientifically analyze, evaluate and compare the performance of multi-antenna mobile handsets with different antenna types and user cases.

# Acknowledgments

We would like to thank our examiner Dr. Buon Kiong Lau and our supervisor Ivaylo Vasilev for their valuable comments and suggestions during the planning and implementation of this thesis project. We are grateful for their help and support throughout the project. This project would not have been completed without them taking the time in guiding us and aiding us with their insightful comments. We also thank Zachary Miers for his kind assistance in some parts of the project. Finally, we would like to thank our family for their support.

Hayder & Baydai

# Table of Contents

# 1 Introduction

## 1.1 Background

The term “user interaction” refers to the interference or coupling between the electromagnetic field of antennas in wireless devices and the human biological tissue (see Fig. 1). User interaction will have more effect on MIMO terminals because the effect of user interaction increases with increasing number of antennas on the terminal.

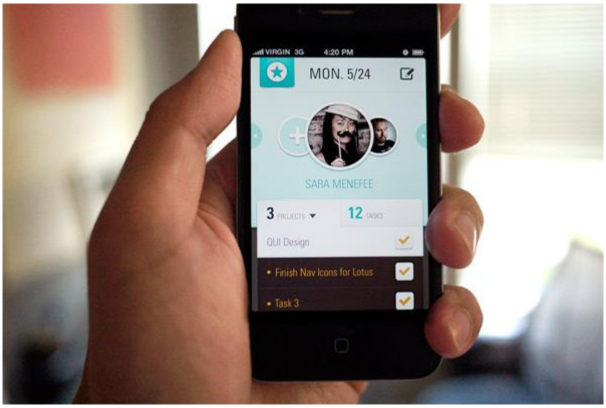


Fig. 1. User interaction

User interaction on a MIMO terminal antenna has been a very interesting research topic in the field of antenna design. From an antenna designer's point of view, it is very important to get an understanding of how the antenna parameters will change with user interaction and under different scenarios of mobile terminal usage. By getting a deeper understanding of the antennas’ behavior in different user interaction cases, we learn how to optimize mobile terminal performance in multiple usage conditions. To our knowledge only few research groups have been or are currently working towards the development of a statistical model that can describe MIMO antenna performance with different user interactions under different user scenarios. Such a statistical model will aid antenna designers in getting a good understanding of antenna performance under different user interaction scenarios. For example, if we have a statistical model that describes the radiation efficiency behavior for different kinds of MIMO antennas with different user interaction scenarios, this will enable engineers and researchers to study link budget using the model. Moreover, antenna engineers will be able to directly use the knowledge of user interaction to design more robust antennas with less severe user interaction issues.

The use of the MIMO techniques in mobile terminals poses many challenges for antenna engineers. One major challenge is to configure multiple antennas in the small sized mobile terminal and get a higher performance. The design of multiple-antenna systems in a smaller area is complicated when taking into consideration coupling and correlation between the antennas. Moreover, user interaction with multi-antenna terminals is an additional significant issue for antenna engineers. Nowadays, mobile phones are designed for different purposes such as phone calls, text messaging, internet access, e-mail access, and so on. With all these different purposes, the grip of the mobile terminal in different positions like “talk mode” or “data mode” strongly depends on the usage. Different hand grips or device orientations must be given great attention in the antenna design because these will have a very significant effect on the antenna performance.

## 1.2 User Interaction

It has been established that the MIMO performance of terminals changes with user interaction from hands, head and body [13]-[17]. In such cases there is high electromagnetic energy coupling between the antenna and the user. This coupling is often located in the near-field region and it leads to the absorption of radiated energy by human tissues. User interaction causes different changes on different antenna parameters; for example, it can change the antenna impedance and therefore detune (mismatch) the terminal antenna [14]. Moreover, user interaction reduces antenna efficiency and modifies antenna radiation patterns, due to absorption losses in human tissues. These effects will consequently reduce the overall antenna performance [14].

Depending on the position of the mobile relative to the hand and head, the influence of a user can differ for various antenna types. User interaction effects can be clearly seen in measurement or simulation results of mobile terminals with head and hand. The results of different user scenarios depend on the grip style [15]. To get better antenna characteristics in the design phase and the best performance in reality, it is necessary to perform a detailed study of how the antenna parameters change with user effects.

In this study, we have designed various grip styles to mimic the holding of a mobile terminal by a user in practice. The two main user scenarios are the talk mode and the data mode. When the terminal is held next to the head, the scenario is called the talk mode; and when the user holds the mobile phone in different grips for utilizing other functions of the mobile device besides making a call, the scenario is called the data mode. In both the talk mode and the data mode, there are many different types of user grips or device orientations that depend on the different usage of the mobile. The interaction between the user and the terminal gives different effects depending on which type of user case is applied and which antenna parameters are affected.

## 1.3 Objective

The major goal of this master thesis is to evaluate and compare the influence of user interaction on different types of antennas in a MIMO communication setup. Moreover, these results will be used to build a statistical model for the different interactions between the user and the different kinds of antennas.

In this project, five different kinds of MIMO prototypes will be used, and each prototype is loaded with ten different user scenarios. The frequency bands used in this project are LTE Band 2 (0.824-0.896 GHz) and LTE Band 5 (1.850-1.99 GHz) [1]. In order to analyze the difference in performance of the antenna parameters, CST (Computer Simulation Technology) Microwave Studio [2] was used to simulate the different antennas in different user scenarios. Two additional programs (Make Human and Blender) were used to design and implement the different user scenarios to be used in CST Microwave Studio.

# 2 Theory

## 2.1 MIMO Overview

Multiple-Input Multiple-Output (MIMO) is a technique that enables increases in data rate and link reliability by using multiple transmitters and receivers to send/receive data simultaneously [3], as depicted in Fig. 2. Today, MIMO is already an integral part of various wireless communication standards (LTE, IEEE802.11n, etc.). The use of MIMO techniques in mobile terminals is a big challenge to antenna designers because of the small size of todays' terminals and additional considerations of multiple antennas such as mutual coupling and radiation pattern correlation. The next chapter in this thesis will discuss in more detail the most significant multiple antenna system performance parameters.


Fig. 2. MIMO principle

## 2.2 MIMO Antenna Parameters

**Pattern correlation** describes the relationship between two antennas when sending or receiving signals through their respective radiation patterns. It specifies the level of similarity between the radiation characteristics of the antenna elements. Correlation decreases the performance of MIMO antennas by reducing the capacity and diversity performance of the antenna systems [4].

**Scattering (S) parameters** are among the important antenna parameters that demonstrate the relationship between the input/output ports of the terminals. They describe the reflection and coupling characteristics of the antennas over a given frequency range. [5].

**Antenna Impedance** is a parameter describing the relationship between the voltage and the current at the input of the antenna. The antenna's impedance consists of two parts: a real part and an imaginary part. The real part is linked to the power that is radiated or absorbed by the antenna. The imaginary part shows how much power is stored in the near field of the antenna. Another parameter that relates to antenna impedance is antenna mismatch (as indicated by reflection coefficient, which is a scattering parameter). It shows how far the antenna impedance is from the matched impedance of the transmission line [5], [6].

**Radiation efficiency** explains the relationship between radiated power from the antenna compared to how much power is actually delivered to the input of the antenna. From equation (1) we can see that the radiation efficiency will be higher when a higher percent of the input power is radiated from the antenna.

$$\eta_R = P_{radiated} / P_{input} \quad (1)$$

where $\eta_R$ is the radiation efficiency, $P_{radiated}$ is the power radiated from the antenna. $P_{input}$ is the power fed to the antenna. Moreover, the relationship between the radiation efficiency and the antenna mismatch efficiency is called **total efficiency** [5], as shown in equation (2)

$$\eta_T = \eta_M * \eta_R \tag{2}$$

where $\eta_T$ is the total efficiency and $\eta_M$ is the mismatch efficiency.

**Radiation pattern** is a parameter that gives details of how the radiated power is spatial distributed in the far-field region. In other words, it shows how the antenna radiates the power that is delivered to it as a function of direction. Different antenna types give different radiation patterns, depending on the current distributions on the antennas [5], [6].

**Antenna bandwidth** shows the frequency interval in which the antenna fulfills a specified requirement, most commonly in terms of maximum reflection coefficient (e.g., -6 dB for terminal antennas) [5], [6].

Currently, there are different kinds of antennas that are used in mobile terminals. The right choice of antenna for a specific mobile device depends on various factors such as the location of the antenna in the device, the size of the mobile, and so on. In general, antennas are divided into five general groups, i.e., wire, microstrip, aperture, traveling wave and log periodic antenna. However, at the same time there are a lot of antennas that are derived by the integration of one or more antenna types in order to accomplish the required performance [7].

## 2.3 Prototypes

In this project, different mobile terminal prototypes are used to study MIMO performance with user interaction. These prototypes are largely based on existing designs, with minor retuning where needed. Current smartphone sizes are used as a guide in the design of the antennas and chassis. Different combinations of antennas are used in different prototypes having the same overall volume of 130×66×8 $mm^3$. In the different prototypes, the antennas were mounted at the edges of the chassis, as is common in terminal antenna design, except for Prototype 3. Five prototypes have been simulated with CST Microwave Studio in free space and with different user scenarios.

### 2.3.1 Prototype One (two IFAs)

The first prototype, which is based on inverted-F antennas (IFAs), consists of two dual-band IFAs located on the edge of the chassis [13], as shown in Fig. 3. IFAs are quite commonly used in wireless communication systems, due to their radiation properties. The name "inverted-F antennas (IFAs)" refers to the antenna structure, which has an inverted F shape, as shown in Fig. 4.

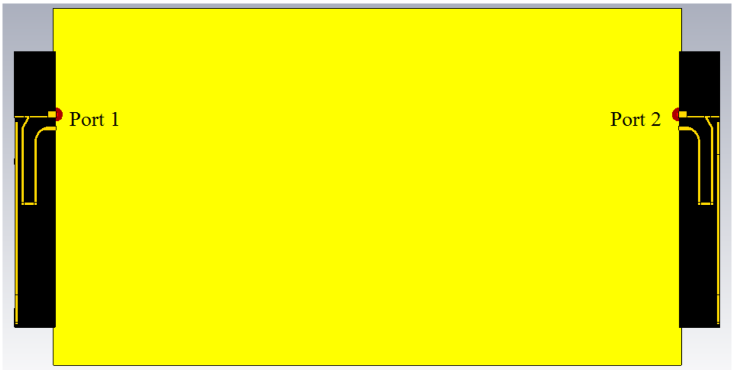


Fig. 3. IFA Prototype

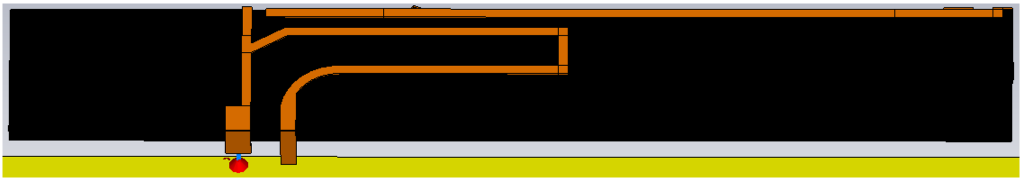

Fig. 4. Enlarged view of the IFA structure

Figure 4 illustrates the IFA structure. The antenna feed pin is indicated by the red marker in Fig. 4. The shorting pin is located on the right of the feed point. Each of the two IFAs has a radiation pattern similar to the classic dipole's donut-shaped pattern. The IFA's performance depends on the length of the upper part, location of feed point and the height of the shorting pin. Both current and voltage distributions of the IFAs are similar to those of a slot antenna, thus resulting in the good performance that the IFA has in terms of radiation pattern and impedance matching [5], [6].

In Prototype One, both IFAs are perfectly mirror symmetric. They have the same structure and dimensions. The IFAs' shorting pin height is 3 mm and the width is 1 mm, whereas the distance between the shorting pin and feed pin is 1.6 mm.

Both IFAs are resonant with sufficient bandwidths at 0.860 GHz for the lower band, and 1.920 GHz for upper band, as shown in Fig. 5, so as to fulfill the requirements of LTE Bands 2 and 5.

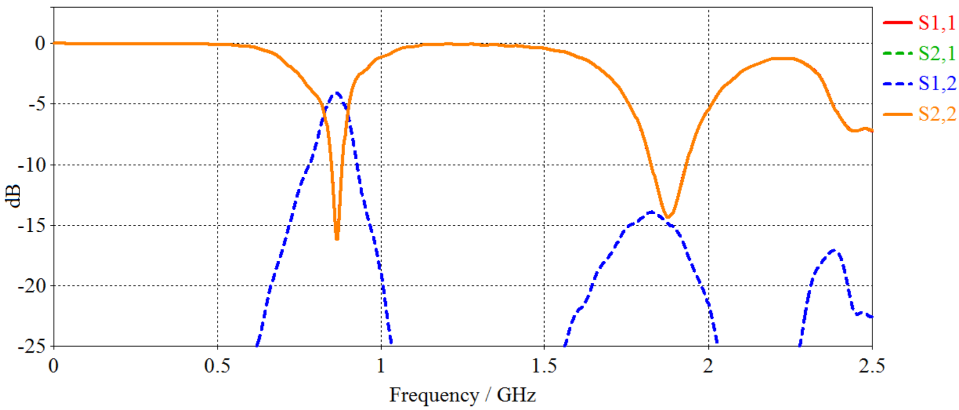


Fig. 5. S parameters for the IFA Prototype in free space

### 2.3.2 Prototype Two (PIFA-Monopole Antennas)

The second prototype in this project has a PIFA-monopole antenna configuration. Antenna one is a planar-IFA (PIFA) and antenna two is a monopole. Each is placed on a short edge of the chassis. The PIFA is placed on the top edge of the chassis while the Monopole antenna is placed on the bottom edge of the chassis. Figure 6 shows the structure of this prototype.

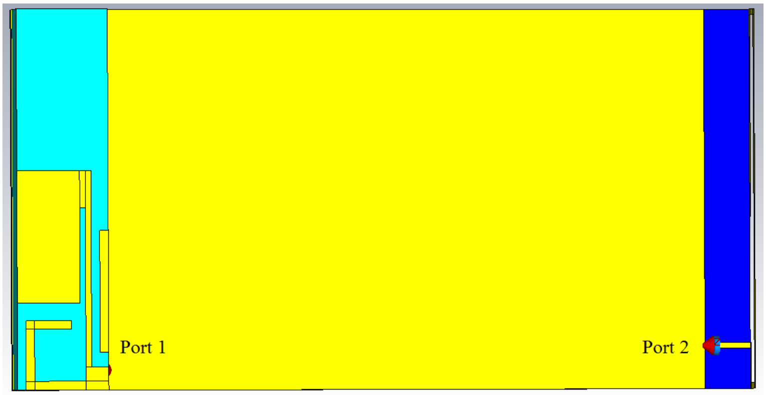

Fig. 6. PIFA-Monopole Prototype

PIFA is one of the most common types of antennas used in mobile terminals. PIFA is an enhanced version of a patch antenna with the addition of a shorting pin that enables a much better performance. PIFA is very popular because of its simplicity in design and its high performance. Moreover, the PIFA radiation pattern is nearly omni-directional, meaning it radiates equal power in almost all directions. The performance of PIFAs is dependent on different parameters like the length and width of the entire antenna, as well as those of the shorting and feed pins. The reduction in the length or width of the antenna will reduce the antenna bandwidth, whereas the resonance frequency of the PIFA depends on the width of the shorting pin. Furthermore, the distance between the feed and shorting pin controls the PIFA impedance [5], [6]. Figure 7 shows the PIFA structure (based on [14]), with the blue box representing the antenna carrier.

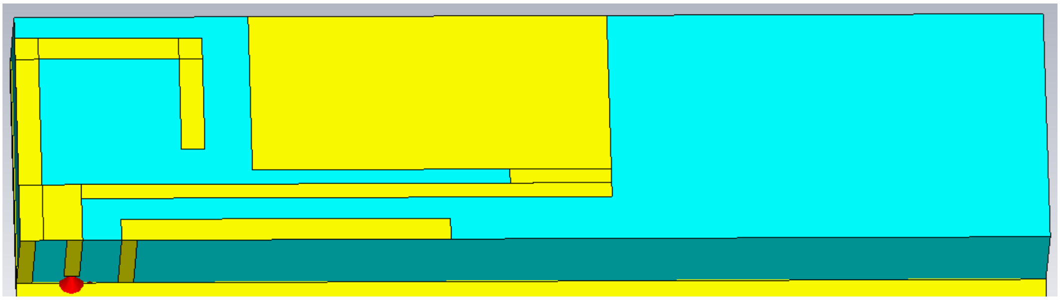

Fig. 7. PIFA structure

The monopole antenna is one of the simplest antennas and also a very common one. The length of the monopole should be equal to a quarter wavelength of the particular resonance frequency. The monopole also has a near omni-directional radiation pattern [5], [6]. The monopole used in this project is shown in Fig. 8.

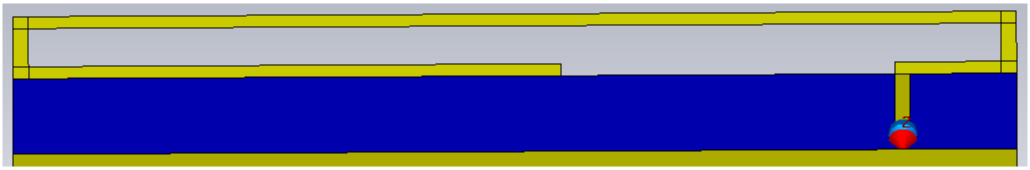

Fig. 8. Monopole antenna structure

As shown in Fig. 6, the PIFA is mounted on a rectangular antenna carrier with the dimension of $66 \times 16 \times 6$ mm$^3$. The shorting pin has a width of 6 mm, whereas the feed point width is 1 mm, with a distance of 2.5 mm between them. Figures 6 and 7 show the structures for both the PIFA and monopole antennas. A lumped element has been added to the feeding port of the monopole to get a better resonance at the lower frequency band.

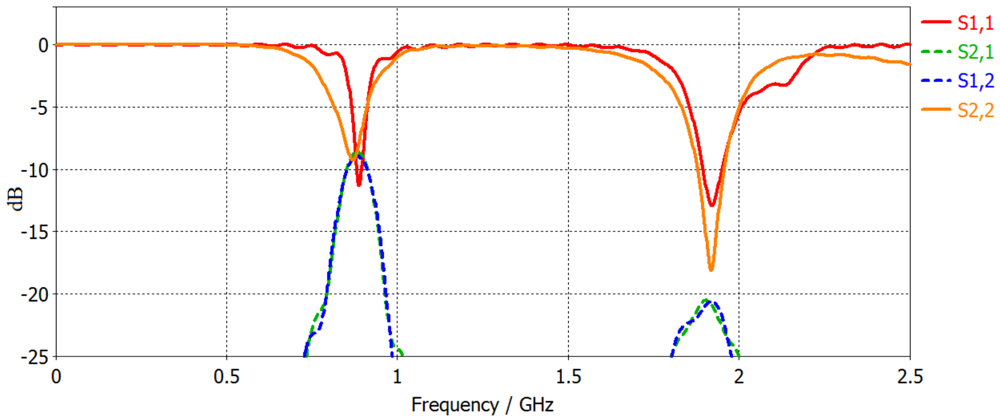


Fig. 9. S parameters for the PIFA-Monopole prototype in free space

Figure 9 shows the S parameters for Prototype Two. From this figure, it is observed that the PIFA has a very small bandwidth in the lower frequency band. This characteristic is a result of the PIFA structure, which imposes more localized current distribution. This prototype has been chosen to reduce the coupling between the antennas by using two different antennas that belong to different antenna families with different mechanisms of operation.

### 2.3.3 Prototype Three (Two Capacitively Fed Antennas)

The third prototype that has been chosen consists of two capacitively fed dual-band antennas [8], as shown in Fig. 10.

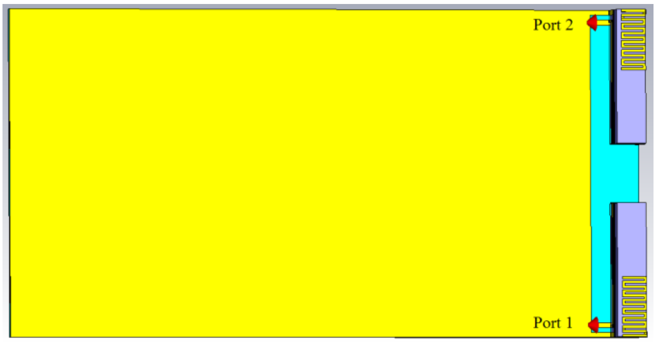


Fig. 10. C-Fed Prototype

The C-Fed (capacitive-fed) antenna can be considered as a long dual-band conductor monopole antenna. The C-Fed antenna consists of a ‘driving element’ that goes alongside a parasitic element, which gives a big advantage in terms of the required length of the monopole. To create a resonance in both the lower and higher frequency bands, each end of the dual-branch driving element is coupled to one of the parasitic ends. The C-Fed antenna has many different parameters that control the resonance frequency in both the lower and upper bands, including the length of the monopole, the distance between the driving and parasitic element and the size/location of the shorting/feed pin. To control the resonance frequency in both bands, a very clear understanding of how the current is distributed on the different parts of the C-Fed antenna is necessary [8].

The two antennas are placed symmetrically on the same short edge of the chassis in order to conserve implementation space and reduce cabling requirement. The structure of the antenna element is shown in Fig. 11.

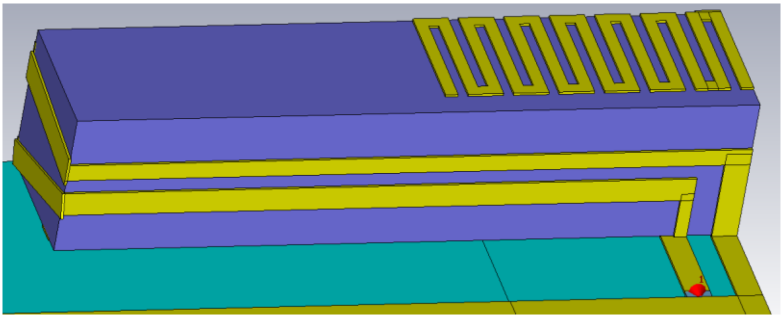

Fig. 11. C-Fed antenna structure

Both C-Fed antennas with meandering ends are placed on rectangular carriers with the dimensions of 27×6×6 $mm^3$. Figure 12 shows the S parameters of the C-Fed antennas, it is clearly seen that each of the C-Fed antennas has a very wide resonance bandwidth, especially in the upper frequency band.

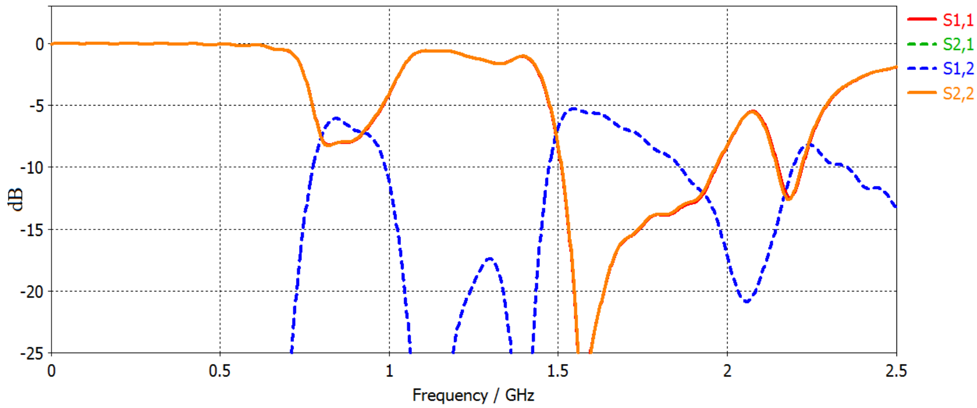


Fig. 12. S parameters for C-FED in free space

### 2.3.4 Prototype Four (T-Shape-Monopole Antennas)

The fourth prototype chosen in this project consists of two different types of dual-band antennas [9]. The first antenna is a T-shape antenna while the second one is a broadband monopole antenna, as shown in Fig. 13. The design of this dual-antenna prototype relies on the use of theory of characteristic modes to generate low coupling and correlation between the two antenna elements [9]. The T-shape and the monopole excite orthogonal modes of the chassis, leading to very low correlation and coupling.

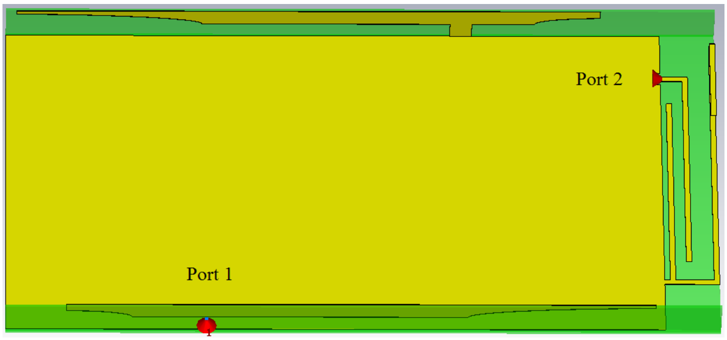


Fig. 13. T-Shape-Monopole Prototype

The T-shape antenna is a novel antenna that has a relatively wide bandwidth in both the lower and upper frequency bands. It consists of two T-strip metal structures located on the opposite long edges of the chassis.

Both metal strips are connected to the chassis through a shorting pin (hence the T-shape). The location and size of the shorting pin have an important role in changing the resonance in both bands. The distance between the feed pin and shorting pin is also an important design parameter. The length of both T-shaped strips is 107 mm, whereas the width and the height from the chassis vary along the length of the strip due to tapering [9].

Fig. 14. Side-view of T-strip antenna

Whereas the T-shaped antenna is located on the long edges of the chassis, the monopole antenna is located on one short edge of the chassis. The two antennas have very low coupling between each other in both the lower and upper frequency bands. Figure 15 shows the S parameters of this prototype in free space.

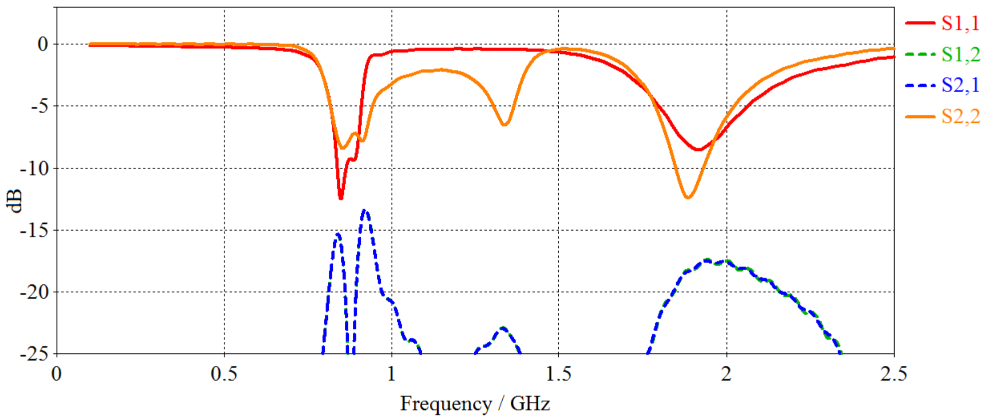


Fig. 15. S parameters for T-Shape-Monopole in free space

## 2.3.5 Prototype Five (Bezel)

The last prototype chosen in this project is the Bezel Prototype. This terminal antenna is based on a very recent study presented in [10]. The Bezel antenna consists of a bezel ring and chassis that is connected via the two ports, as shown on Fig. 16. Each of the two ports is connected to a piece of metal that is in turn connected to the bezel ring. The first metal piece is connected to the long edge of the bezel ring whereas the second one is connected to the short edge of the bezel. The dimension of the bezel ring is 130×66×8 $mm^3$.

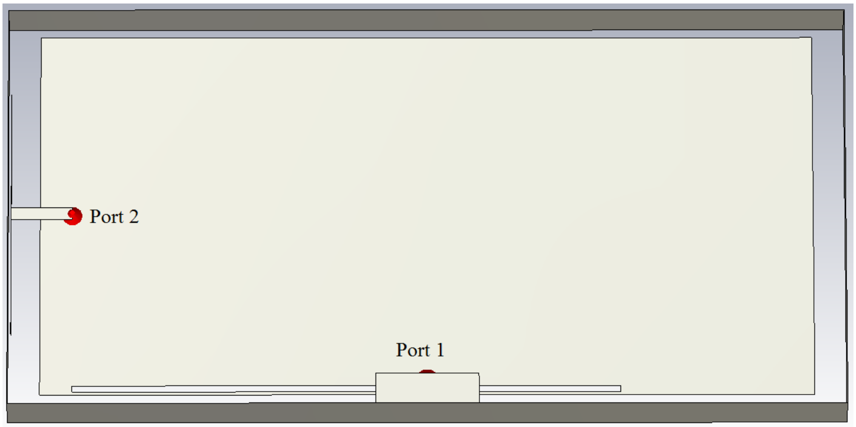


Fig. 16. Bezel Prototype

The Bezel Prototype closely follows the design method used for Prototype Four, where the performance depends on the different chassis excitation modes employed. The S-parameter performance of the Bezel antenna in free-space is shown in Fig. 17. The Bezel antenna has a very lower correlation in both bands and achieves very good efficiency in terms of both total and radiation efficiencies [10].

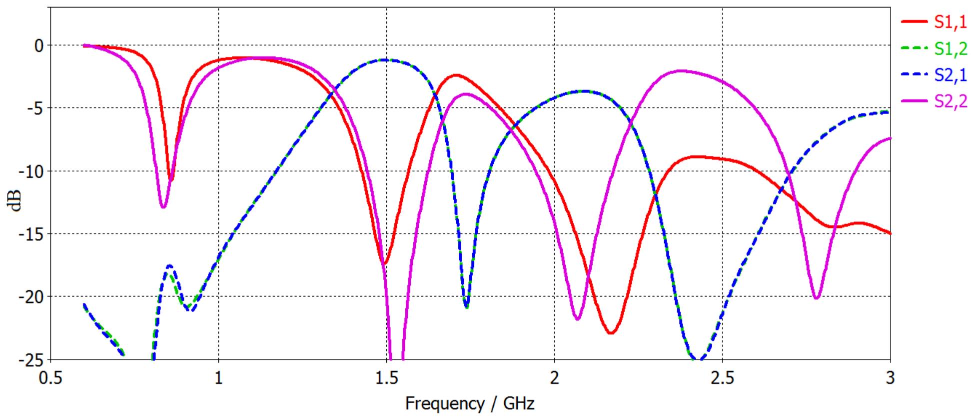

Fig. 17. S parameters of Bezel Prototype in free-space

## 2.4 MIMO System Performance

In this project, we calculate some of the most common MIMO performance metrics to evaluate the different antenna prototypes and to gain a deeper understanding of how these performances change under different user scenarios.

### 2.4.1 Multiplexing Efficiency

Multiplexing efficiency describes the absolute efficiency of a MIMO antenna, taking into account non-ideal behavior in both total efficiency and correlation [12]. It defines the equivalent loss of power efficiency when using a practical MIMO antenna to achieve the same channel capacity as that of an ideal MIMO antenna in the same propagation channel (e.g., uniform 3D angular power spectrum [12]).

### 2.4.2 MIMO Capacity

Channel capacity is defined as the maximum error-free data rate that the channel can support. By using MIMO techniques the capacity increases in a very significant way [11], [13]. In this project, we investigate MIMO capacity based on the Kronecker channel model.

By assuming a 2×2 MIMO system with no channel state information, the capacity can be expressed as [12]:

$$C = \log_2 \det(\mathbf{I}_2 + P_\mathrm{T}/2\ \mathbf{H}\mathbf{H}^H) \tag{3}$$

where **H** is the MIMO channel matrix, $\mathbf{I}_\mathrm{M}$ is the 2×2 identity matrix, $P_\mathrm{T}$ is the transmit power and $(.)^H$ denotes the conjugate transpose operator. Assuming that we use the reference propagation environment (independent and identically distributed channel or i.i.d.) with no correlation at the base station antennas, the channel **H** can be calculated as shown below [12]:

$$\mathbf{H} = \mathbf{R}^{1/2}\ \mathbf{H}_\mathrm{w} \tag{4}$$

where **R** is referred to as the receive correlation matrix and $\mathbf{H}_\mathrm{w}$ is the i.i.d Rayleigh fading channel. The received correlation matrix can be calculated by using the following equation:

$$\mathbf{R} = \mathbf{\Lambda}^{1/2}\ \acute{\mathbf{R}}\ \mathbf{\Lambda}^{1/2} \tag{5}$$

where $\acute{\mathbf{R}}$ is the normalized correlation matrix (with ones along its main diagonal) and $\mathbf{\Lambda}$ is a diagonal matrix defined by

$$\mathbf{\Lambda} = \mathrm{diag}[\eta_1,\ \eta_2] \tag{6}$$

where $\eta_\mathrm{i}$ is the total efficiency on the *i*-th antenna port.

# 3 User Scenario Design

Antenna performance is significantly affected by human tissue in the vicinity of the antenna, due to the tissue's interaction with the antenna's near-field and far-field radiation. This influence can change antenna performance parameters such as antenna radiation pattern, antenna efficiency, antenna mismatch efficiency and antenna pattern correlation. The large variations of human interaction with smartphones lead to numerous possible hand grip styles. Different grip styles depend on how many hands are used to hold the phone and on the positions of the palm and fingers. Furthermore, user interaction will also depend on which mode the mobile is used in. Mode refers to the purpose of the phone's usage. The two general modes are talk mode (TM) and data mode (DM). In the TM, the mobile is typically placed close to the head and the main usage scenario is phone calls. This mode has different grip styles depending on the position of the hand and the orientation of the device with respect to the head and hand. In the DM, the phone is typically placed in a hand-held position with usage scenarios varying from browsing with one or two hands to gaming and watching videos [15].

## 3.1 Design Software

The different user scenarios investigated in this thesis have been designed and implemented in two open source programs (MakeHuman 1.0 Alpha 7 and Blender). Screenshots from these two programs are shown in Figs. 18 and 19.

Both software tools enable the design of 3D objects in a very intuitive way. In MakeHuman we were able to design a virtual homogenous human hand with realistic dimensions. Unfortunately, MakeHuman does not provide flexibility in changing finger or palm positions and therefore does not suffice to generate diverse user scenarios. The second software used in the design process (Blender) solved this problem and allowed for flexible hand models to be used and therefore the desired fundamentally different user scenarios to be designed.

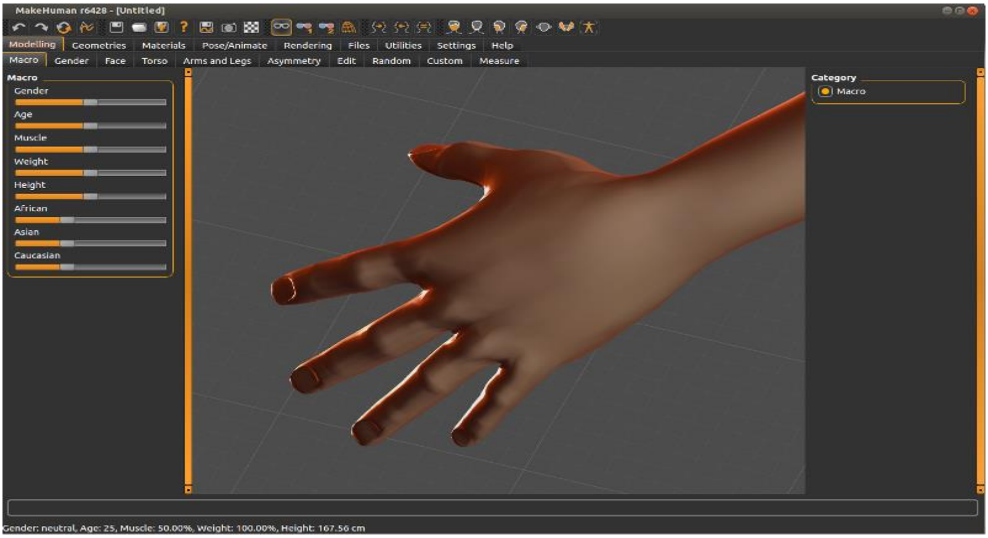

Fig. 18. MakeHuman program

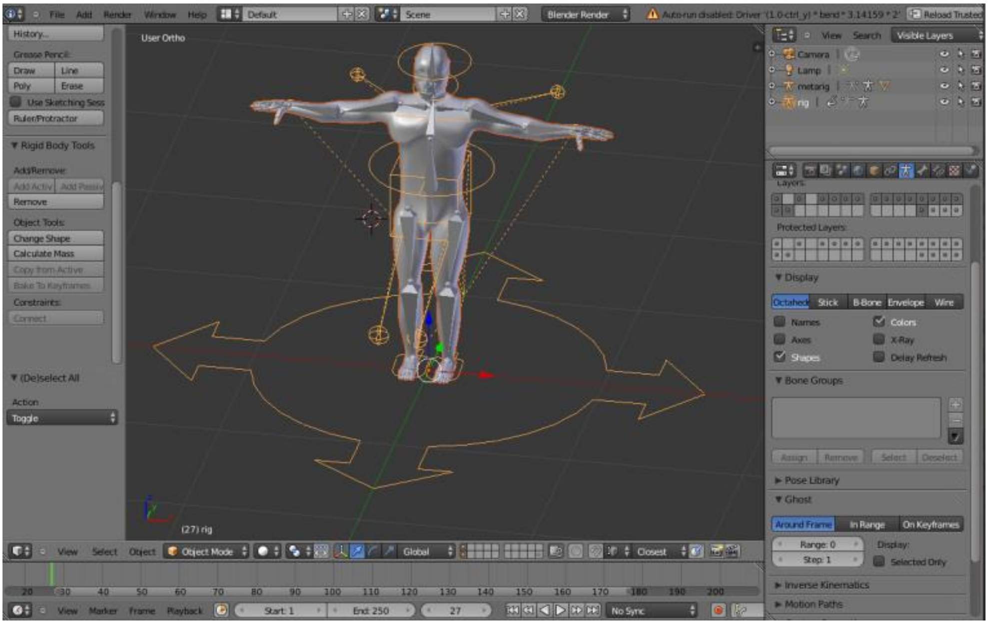

Fig. 19. Blender program

## 3.2 User scenario

In this project we investigated in detail two main user scenarios (TM and DM) and their variations depending on the smartphone usage and the dimension/position of the terminal with respect to the user.

### 3.2.1 Data Mode (DM)

In the following subsections we present the DM cases studied in this thesis project. They are divided into one-hand and two-hand cases.

#### 3.2.1.1 One-Hand Design

Many people operate their smartphones with one hand when using the terminal for browsing, texting, sending/receiving e-mail or watching videos. The one-hand DM is divided into two main usage/grip styles:

***One-Hand Browsing Mode (1HB)***

This grip is one of the most common human grips when using a mobile phone for different purposes like writing a text message (mail or SMS) or browsing the phone when using different types of online applications. The grip is shown in Fig. 20.

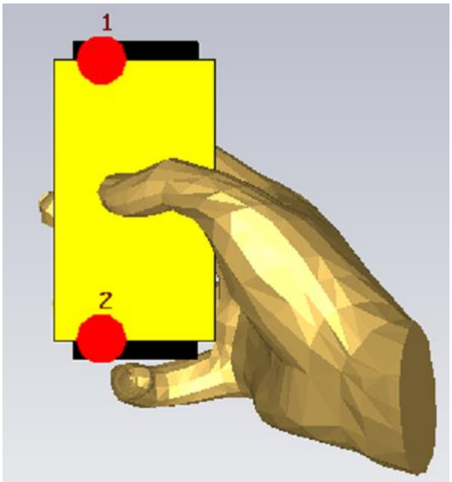


Fig. 20. One-Hand (OH) Browsing Mode

In this grip the middle three fingers provide support at the back of the phone, whereas the little finger sits under the mobile for bottom support. The thumb of the holding hand is used for browsing on the screen of the terminal [9], [16].

***One-Hand Video Mode (2HV)***

This mode is similar to the first grip, but in this case the thumb of the holding hand is placed on the side of the mobile to give more space to the user to view the screen. Fig. 21 shows the grip in detail [16].

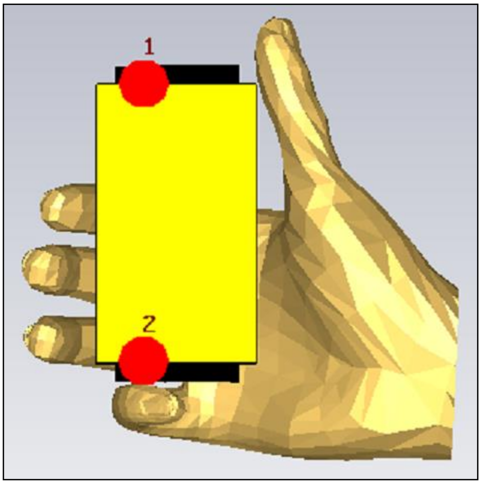


Fig. 21. One-Hand (OH) Video Mode

#### 3.2.1.2 Two-Hand Design

Nowadays, a lot of terminals are used with two hands due to the increase in terminal size. In this project, different types of user scenarios involving two hands/landscape cases have been studied. The landscape orientation is considered as one of the worst case scenarios in the DM due to the presence of two hands at the same time. The two hands DM has been designed in this project with five different hand grips.

### *Two-Hand Browsing Mode (2HB)*

This hand grip is the third grip in our study. In this grip the user holds the phone with two hands and the thumbs are used for browsing, as shown in Fig. 22. The thumbs are placed in front of the screen, whereas the middle three fingers on both hands are placed behind the phone to hold it in position. The little fingers on both hands are placed under the longer edge to support the terminal [9].

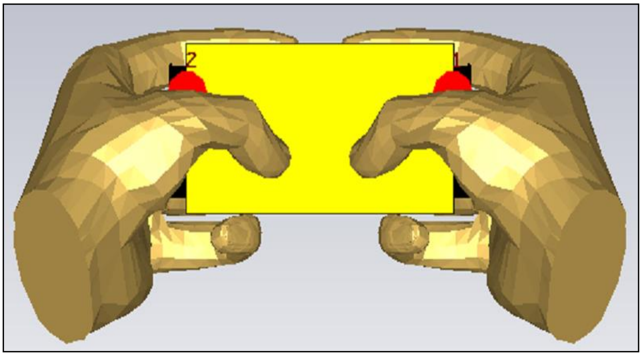

Fig. 22. Two-Hand (TH) Browsing Mode

### *Two-Hand Video Mode (2HV)*

In this grip the thumbs are placed on the side of the mobile. This grip is very popular when watching online movies or when talking in a video call. Fig. 23 shows the positioning of this grip [17].

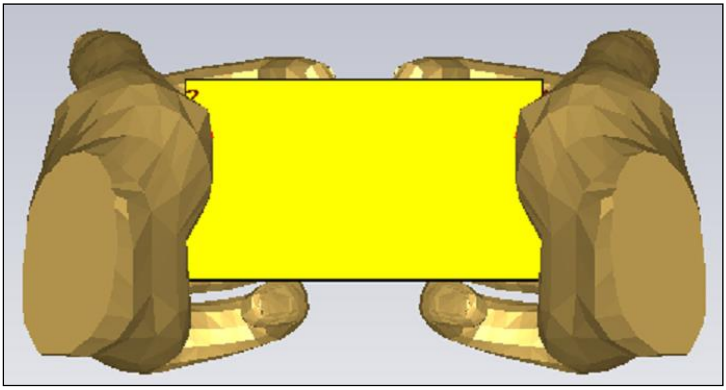

Fig. 23. Two-Hand (TH) Video Mode

***Two-Hand-Around Browsing Mode (2HAB)***

This grip is one of the most interesting grips that have been added to the project, due to the fact that in this particular scenario the terminal is surrounded from almost all directions with human tissue. It is based on observations of different people when they used a wide sized terminal. Further, this grip is also partly based on the studies in [16]. The positioning of this grip is given in Fig. 24. Two hands are used to hold the terminal while the index fingers are folded around the longer side.

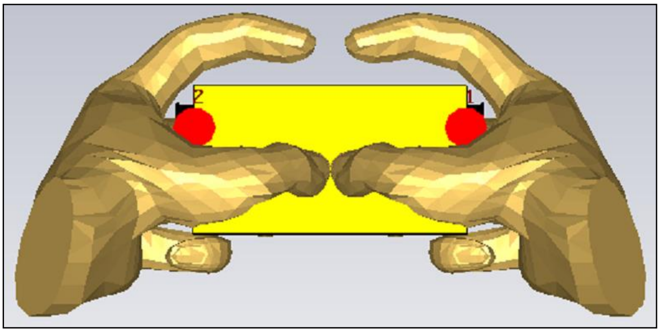

Fig. 24. Two-Hand (TH) Around Browsing Mode

***Two-Hand-Around Video Mode (2HAV)***

This grip is similar to the previous grip except for the thumb placement. While the thumbs in the previous grip are used to point to the screen of the mobile, in the 2HAV grip they are placed on the side of the screen to give more viewing space to the user (see Fig. 25).

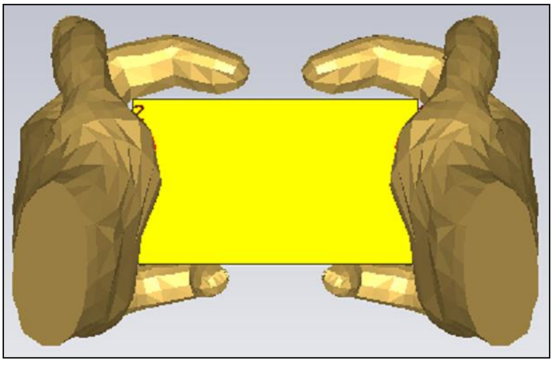

Fig. 25 Two-Hand (TH) Around Video Mode

***Two-Hand Vertical Browsing Mode (2HVB)***

The last grip investigated in this project is the *two-hand vertical browsing mode* with a portrait orientation of the mobile phone. This grip has become very popular in the past years due to the ever increasing smartphone size. Newer generation devices have a long, wide screen which is comfortable to use with two hands not only in the landscape mode but also in the portrait mode. A more detailed snapshot of the grip is shown on Fig. 26. All fingers (except the thumbs and little fingers) are folded around the mobile to help hold the terminal whereas the little fingers are placed under the terminal to support it from the bottom. The thumbs are placed in the front of the screen and are normally used for browsing the device [16].

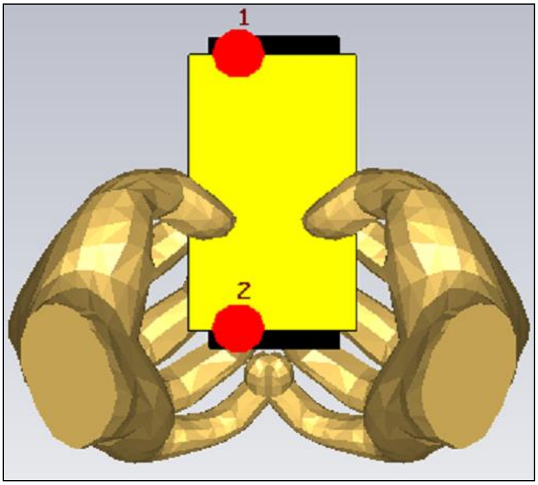


Fig. 26. Two-Hand (TH) Vertical Browsing Mode

### 3.2.2 Talk mode (TM)

To study user interaction in the TM, three different scenarios have been chosen. Figure 27 shows these three different cases in more detail. In all cases the position of the fingers around the terminal is constant, while the orientation of the terminal with respect to the head is changed in steps of 30 degrees from 0 to 60 (see Fig. 27). The handgrip that has been used in those three TM scenarios is *One-hand with index* finger. This particular grip is considered as the typical TM handgrip where the thumb is placed on the longer side of the mobile to support it from one side while the rest of the fingers, excluding the index finger, are folded around the terminal from the other side for support. The index finger is placed on the back of the terminal which gives comfort to the user when the mobile is very close to the ear [18].

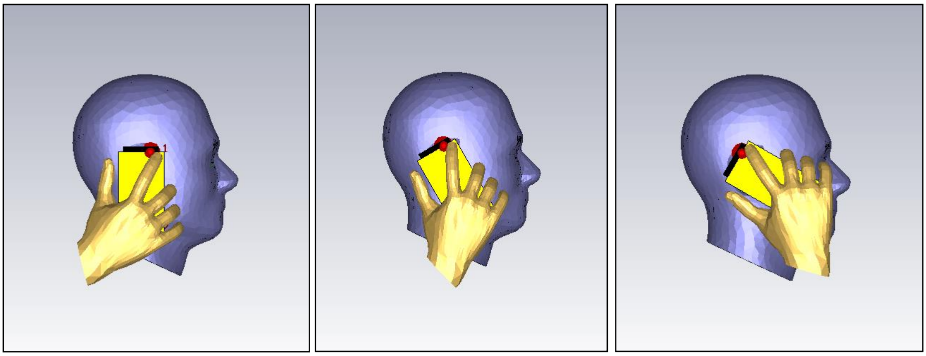

(a) (b) (c)

Fig. 27. TM with three different orientation of the terminal (a) at 0 degree, (b) at 30 degree and (c) at 60 degree.

# 4 Simulation Setup and Results

## 4.1 Setup

2013 CST Microwave Studio was the 3D electromagnetic solver used to run the full-wave simulations of different prototypes with and without user interaction. The simulation performance and runtime were affected by many factors like the number of mesh cells, type of solver, and frequency range. In the beginning of this project a high number of mesh cells was used which led to very long run times. The mesh size was then optimized following discussions with the CST Support Team and through the usage of the mesh-group option which allocated different parts of the prototype into different mesh groups where each group had different mesh properties.

## 4.2 Simulation Results

All prototypes were simulated in CST for three general cases (free space, TM and DM). The simulation in free space was done for the five different prototypes for different reasons. The first reason is to get an understanding of the antenna's performance in free space without any interaction. We consider this as a reference case when comparing the performance of the particular prototype with different user scenarios. The second reason is to demonstrate the conformance of the terminals to the design goals specified by the LTE standard for Bands 2 and 5. The simulation of different user scenarios in both TM and DM was done to gain an understanding of the performance of the different antenna prototypes in different user scenarios. In the following section, we will discuss the simulation results of different prototypes in terms of antenna parameters like S parameters, frequency offset from the resonance frequency, total and radiation efficiencies, mismatch efficiency, capacity and correlation. It is noted that, for clarity of presentation, only the reflection coefficient for the port that is more affected by the user in terms of detuning is shown for the considered user scenarios (i.e., denoted as port 1 for all five prototypes in Section 2.3). Likewise, coupling coefficient is omitted, since it is below -12 dB for all user cases and all five prototypes. For consistency, total efficiency is also shown for port 1 only.

### 4.2.1 Data Mode (DM)

The first part of the results discusses the performance of the five prototypes in the seven DM user scenarios.

#### 4.2.1.1 IFA Prototype

Figure 28 shows the performance of the first prototype (IFA Prototype) from the S-parameter point-of-view with different user scenarios in DM. By comparing the performance of the IFA Prototype in free-space with the performance in the remaining user cases, we can clearly see the impact of user interaction. It affects the antenna performance by causing a frequency offset of the resonance frequency and also variations in bandwidth.

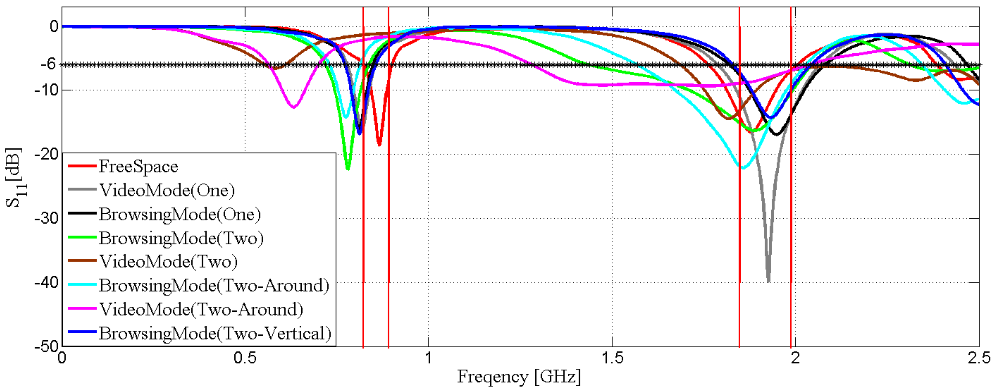


Fig. 28. S parameters for IFA Prototype with different user scenarios

The impact of various user cases is different over all scenarios. These differences depend on the location of the hand and fingers. In Two-Hand Video Mode (2HV), part of the hand's palm and the index finger are very close to the section of the IFA Prototype that is responsible for radiation in the lower frequency band. Due to this proximity most of the radiated power of the antenna is absorbed by these two parts of the hand, which also result in a frequency offset in the resonance frequency. If we now take a look at user case number six, the Two-Hand Around Video Mode (2HAV), we can see the performance of the IFA Prototype affected in both the lower and higher frequency bands. The lower band of the IFA Prototype has a frequency offset of 240 MHz compared to the free-space performance. This offset is due to the fact that the index finger interferes with the radiation pattern of the IFA in the lower band. This, in turn, causes a change in the direction of radiation and a mismatch at the antenna ports. The reason behind the bandwidth expansion in the upper band in user scenario 2HAV is that the part of the IFA Prototype that is responsible for radiation in the higher frequency band is nearly covered from all directions by the hand. This leads to a lot of absorption and mismatch. The impact of this particular user case (2HAV) cannot be considered as advantageous since the radiation efficiency in the entire higher band is very low (18 %).

Table 1 shows the radiation and total efficiencies of an IFA element (port 1) in the IFA Prototype with different DM user scenarios compared to free-space at the center frequency of the lower band. The radiation and total efficiencies vary significantly across the different cases. The reason behind the variations in the total and radiation efficiencies is the different levels of antenna mismatch and absorption in human tissues for the different user scenarios. Further, due to the impact of user interactions we get a significant change in the current distribution of the antennas.

| **User Cases** | **Radiation Efficiency (%)** | **Total Efficiency (%)** |
|---|---|---|
| Free-space | 81,6 | 47 |
| 1HV | 55,5 | 29,7 |
| 1HB | 78,6 | 40,9 |
| 2HB | 30,1 | 15,7 |
| 2HV | 25,1 | 5,1 |
| 2HAB | 43,7 | 15,2 |
| 2HAV | 15,8 | 4,6 |
| 2HVB | 73,3 | 44 |

Table 1 IFA Prototype – total and radiation efficiencies of each IFA element

As noted above, MIMO capacity is a very important metric for prototype evaluation from a system perspective. Figure 29 shows the capacity performance of the IFA Prototype in different user scenarios. Due to the dependence of capacity calculations on correlation and efficiency we present these results in Figs. 29 and 30.

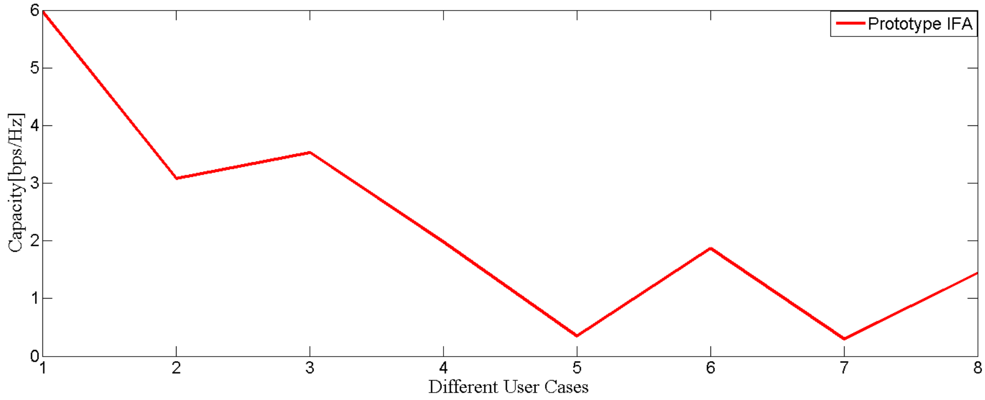


Fig. 29. IFA Prototype – capacity

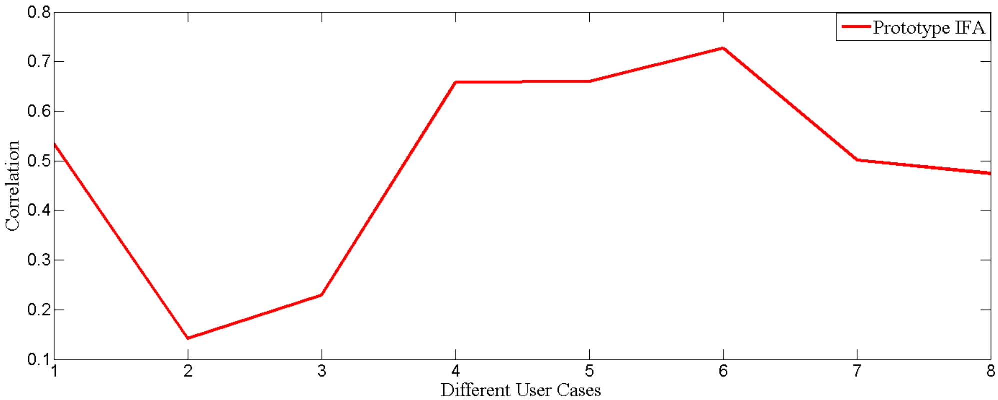


Fig. 30. IFA Prototype – correlation

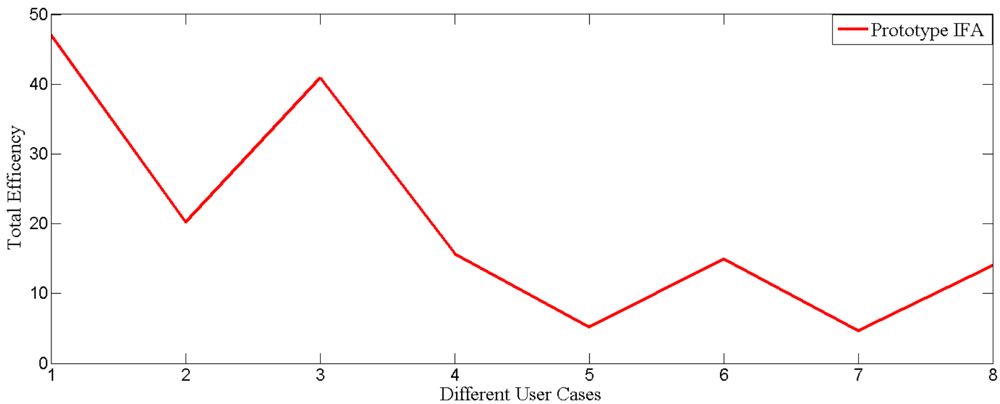


Fig. 31. IFA Prototype – total efficiency

The capacity for user cases 5 and 7 (2HV, 2HAV) is significantly lower than other cases, because in these two particular cases the correlation between the IFA elements is high, as shown in Fig. 30. Moreover, the total efficiency in these two cases is very low (Fig. 29) which contributes to the low capacity.

#### 4.2.1.2 C-Fed Prototype

The S parameters of the C-Fed Prototype in different user cases are shown in Fig. 32. The figure shows how each C-Fed antenna behaves in different user scenarios compared to that in free-space. The C-Fed antenna is considered as a wideband antenna and because of this feature the C-Fed is not severely affected either in terms of frequency offset or in terms of change in bandwidth.

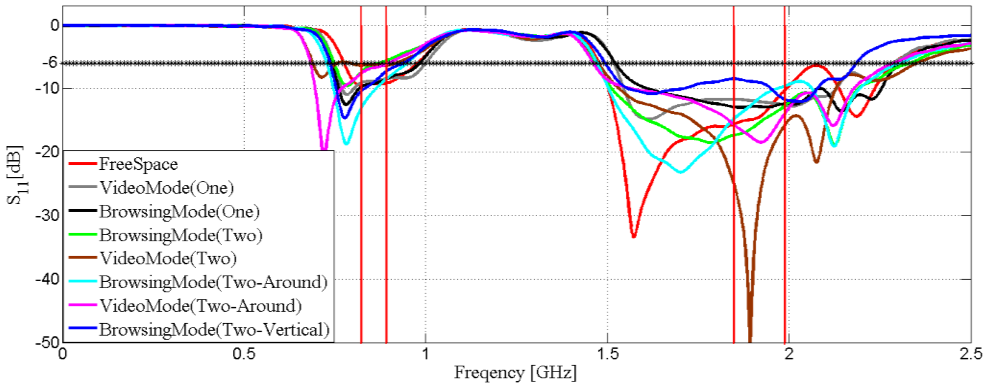


Fig. 32. S parameters of C-Fed Prototype with different user scenarios

The largest frequency offset in the C-Fed Prototype in the lower frequency band was in user cases 2HV and 2HAV at 96 MHz. The reason for this offset in these two particular user cases is that the thumb placement is very close to the section of the antenna that is responsible for radiation in the lower band. Further, in these two certain user cases, both of the C-Fed antennas were covered from all directions by the hand's palm and fingers.

Figure 33 shows the capacity performance of the C-Fed Prototype in the center frequency of the lower band with different user scenarios. In general, the capacity performance of the C-Fed Prototype is better than the IFA Prototype since the C-Fed Prototype has lower coupling between the

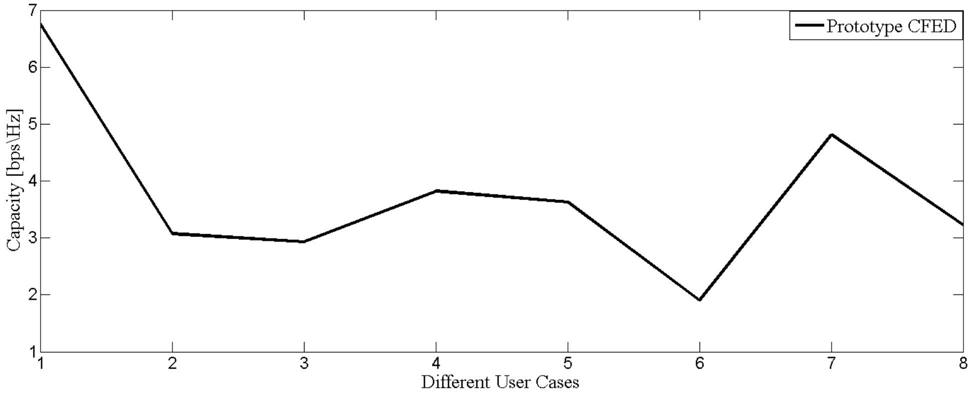


Fig. 33. C-Fed Prototype – capacity

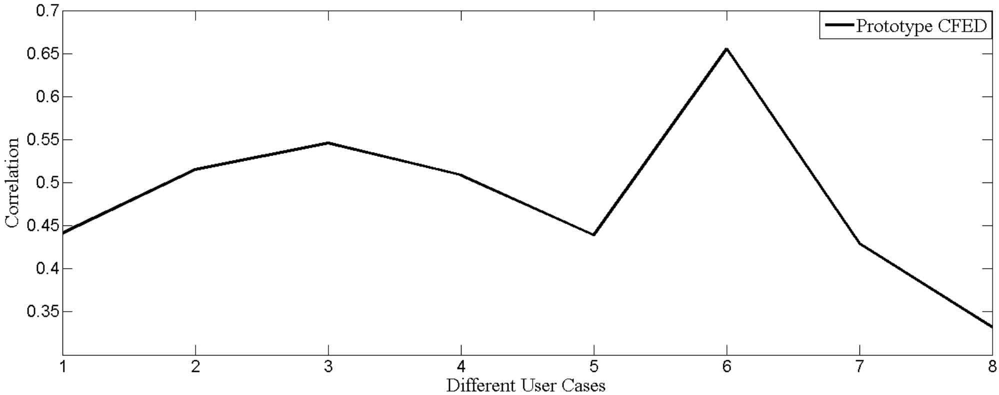


Fig. 34. C-Fed Prototype – correlation

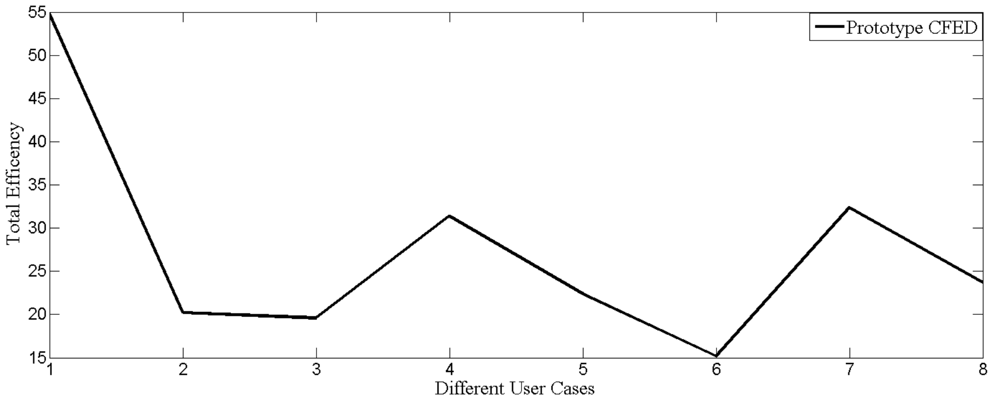


Fig. 35. C-Fed Prototype – total efficiency

antennas and also higher total efficiency compared to the IFA Prototype. The impact of user case number seven (2HAV) gives the minimum user effect from a capacity point of view. In this case the correlation and total efficiency are favorable for a higher channel capacity (see Figs. 34 and 35).

Table 2 shows the performance of the C-Fed Prototype in terms of total and radiation efficiencies at the center frequency of the lower frequency band. The table also shows how the performance of a C-Fed antenna (port 1) with different user scenarios compares to the performance in free-space. The radiation efficiency of the C-Fed Prototype goes down significantly due to the impact of the user's interaction. The C-Fed antenna has lower radiation efficiency with user case 1HB when compared to other user scenarios because, in this particular case, the thumb obstructs the radiation pattern of the C-Fed antenna. This interference by the thumb causes a reduction in the radiation power and therefore efficiency.

| User Cases | Radiation Efficiency (%) | Total Efficiency (%) |
|---|---|---|
| Free-space | 90,8 | 54,8 |
| 1HV | 30,8 | 20,2 |
| 1HB | 28,4 | 19,6 |
| 2HB | 46,6 | 31,4 |
| 2HV | 34,9 | 22,4 |
| 2HAB | 42,9 | 15,2 |
| 2HAV | 47,6 | 32,4 |
| 2HVB | 35,6 | 23,7 |

Table 2 Total and radiation efficiencies of C-Fed Prototype

#### 4.2.1.3 T-Shape Prototype

Figure 36 shows the S parameters of the T-Shape Prototype in different user cases compared to the performance in free-space. It indicates that the T-shape Prototype has better performance than the first three prototypes from two points of view: frequency offset from the resonance frequency and bandwidth stability over different user cases. The low coupling between the two antennas (T-shape and monopole) is the main reason behind the lower impact of users. Furthermore, the radiation pattern of the antennas is directed away from the user influence (e.g., shadowing by fingers) which has a positive effect on the overall performance. From the frequency offset point of view, the largest impact of user interaction on this prototype is in user case 1HV which has a frequency offset of 26 MHz in the lower band. The reason behind this behavior in this particular case is that the thumb is very close to the radiating part of the T-antenna at this frequency which leads to a change in the current distribution in the T-shape antenna.

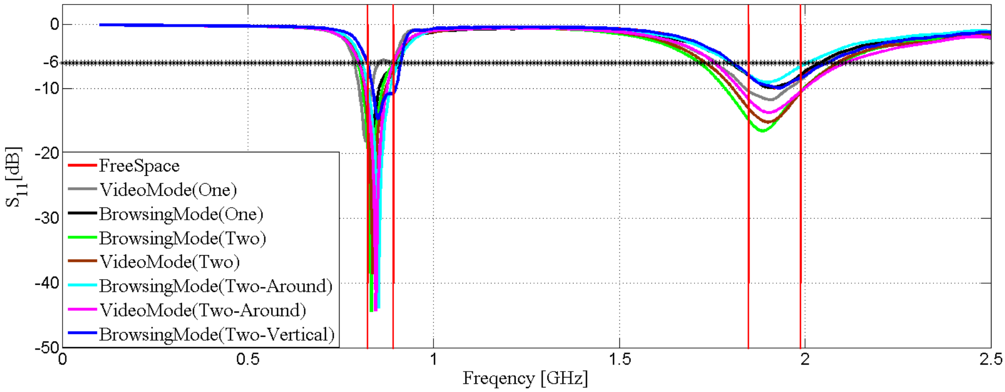


Fig. 36. S parameters for T-shape Prototype with different user scenarios

Table 3 shows the performance of the T-shape Prototype (port 1) from a radiation and total efficiencies point of view in different user scenarios. The user cases tested here have a significant effect on both the total and radiation efficiencies mainly due to absorption losses. The radiation efficiency is mostly affected in the 2HB user case for both the lower and the higher frequency bands.

| User Cases | Radiation Efficiency (%) | Total Efficiency (%) |
|---|---|---|
| Free-space | 97,3 | 87,4 |
| 1HV | 52,1 | 35,3 |
| 1HB | 37,8 | 30,4 |
| 2HB | 29,1 | 25,7 |
| 2HV | 38 | 34,5 |
| 2HAB | 34,9 | 34,6 |
| 2HAV | 31,3 | 30 |
| 2HVB | 50,8 | 44,8 |

Table 3 Total and radiation efficiencies for T-shape Prototype

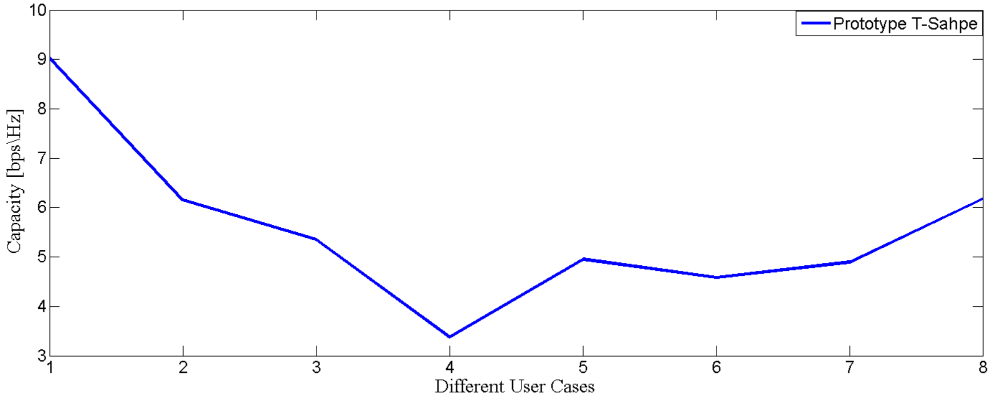


Fig. 37. T-shape Prototype – capacity

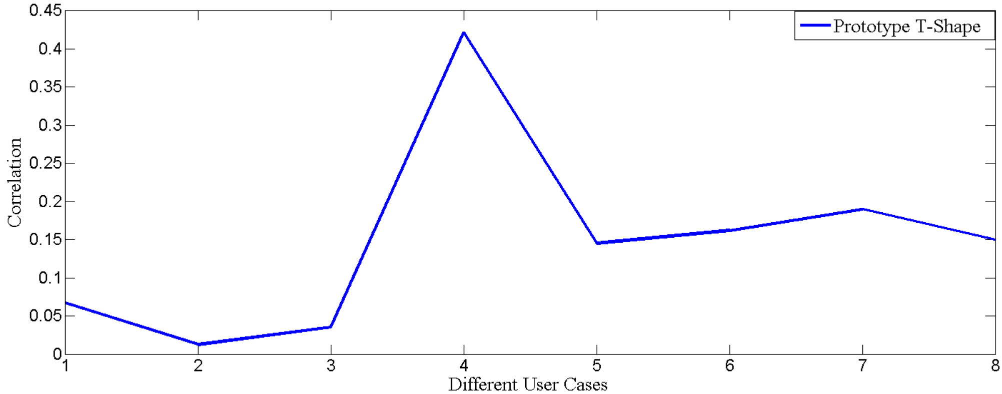


Fig. 38. T-shape Prototype – correlation

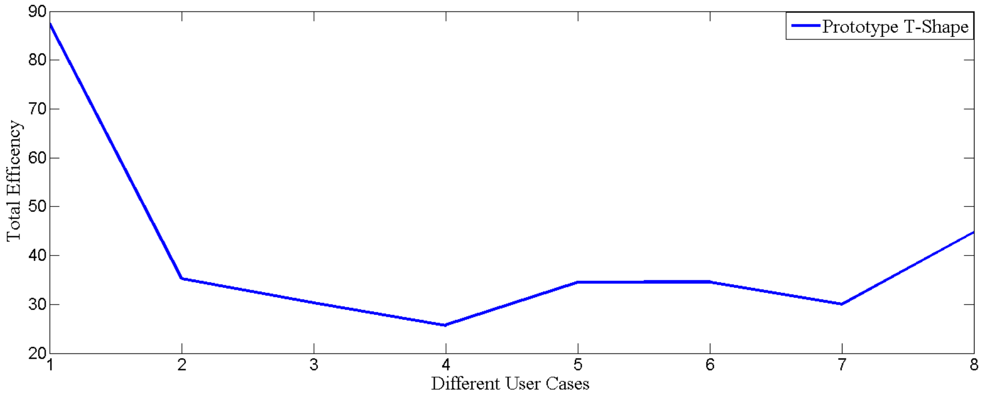


Fig. 39. T-shape Prototype – total efficiency

The capacity performance of the T-shape prototype in different user scenarios is shown in Fig. 37. It has a better performance than the first three prototypes in all user cases. This is due to the favorable behavior of the T-shape prototype in both correlation and total efficiency. The worst case in terms of user impact on the capacity performance of the T-shape prototype is for the 2HB user case. In this case the correlation of the terminal is higher leading to a degraded capacity (see Fig. 37-39).

#### 4.2.1.4 PIFA(-Monopole) Prototype

Figure 40 shows the performance of the PIFA Prototype in terms of S parameters in the different user scenarios. It indicates that the largest frequency offset in this prototype is for 2HB (Two-Hand Browsing Mode) with a frequency offset of 26 MHz in the lower frequency band. The reason behind this small range of the frequency offset compared to the other prototypes is that the PIFA (worse affected by user effects than the monopole antenna, hence shown in Fig. 40) is a very narrowband antenna and the calculation of frequency offset depends on the offset from the center frequency. Also, the figure shows that the PIFA experienced very pronounced detuning in the higher band due to the impact of the users hand in One-Hand Video Mode (1HV). In this particular case, the section of the PIFA located on the side of the prototype that radiates in the higher frequency is very close to the thumb. This placement leads to high absorption of radiation power in the thumb and therefore severe impact on the S parameters.

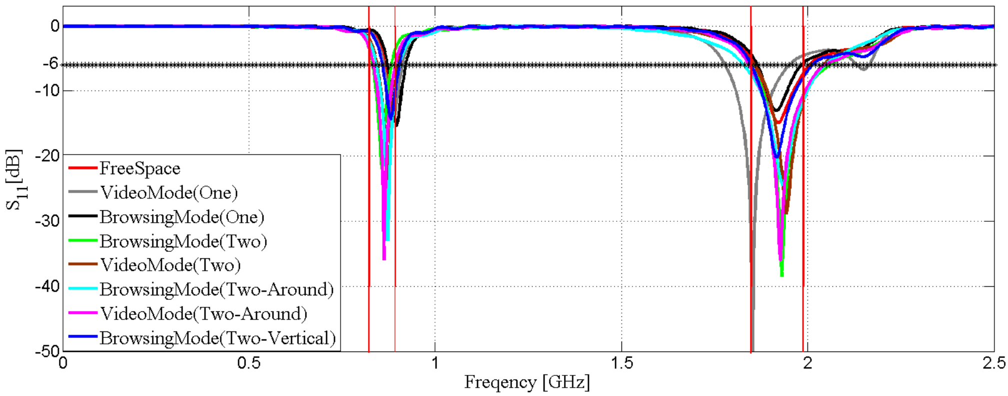


Fig. 40. S parameters of PIFA Prototype with different user scenarios

Table 4 shows the performance of the PIFA element in the PIFA Prototype from two points of view: radiation and total efficiencies. The lowest value of the radiation efficiency of the PIFA is on the lower frequency band with user case 2HB. This low level in the radiation efficiency value is caused by the grip of the user. In this case the PIFA is covered from all directions by the fingers and palm of the hand. Therefore the radiated power is then reflected towards the monopole antenna which then absorbs part of it to lead to higher coupling between the two elements.

| **User Cases** | **Radiation Efficiency (%)** | **Total Efficiency (%)** |
|---|---|---|
| Free-space | 82,2 | 36,4 |
| 1HV | 45,6 | 26 |
| 1HB | 63 | 22,8 |
| 2HB | 36 | 33,3 |
| 2HV | 39,5 | 33,2 |
| 2HAB | 34,9 | 30,5 |
| 2HAV | 41,4 | 37,9 |
| 2HVB | 56,5 | 37,5 |

Table 4 Total and radiation efficiencies for PIFA Prototype

The capacity performance of the PIFA Prototype is shown in Fig. 41. This figure shows that the PIFA Prototype has better capacity performance than the C-Fed Prototype at the center frequency of the lower band. The capacity performance of the PIFA Prototype in different user scenarios varies a lot because both the correlation and total efficiency of the prototype change considerably from case to case, as shown in Figs. 42 and 43.

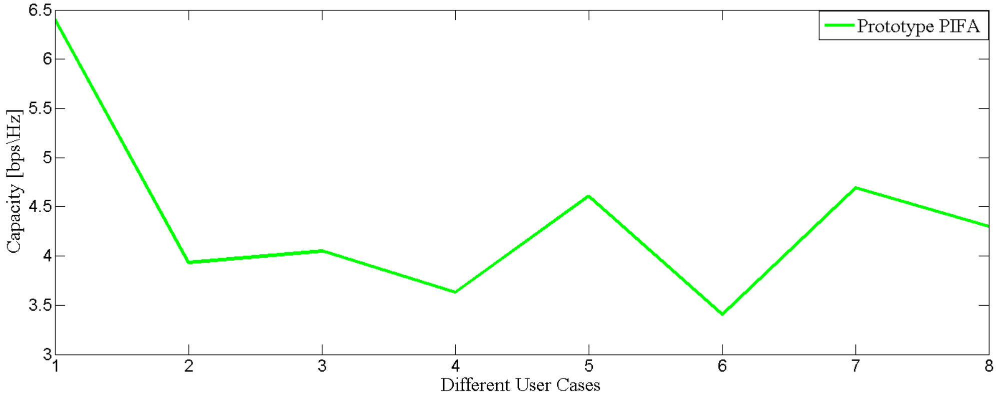


Fig. 41. PIFA Prototype – capacity

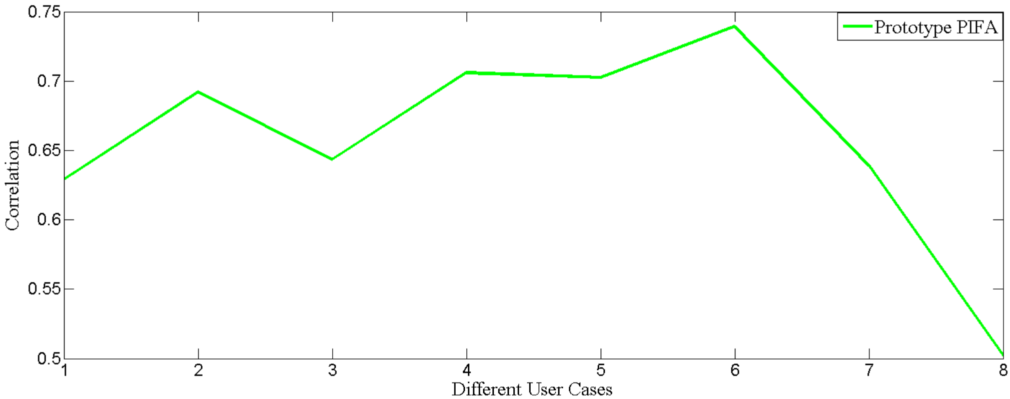


Fig. 42. PIFA Prototype – correlation

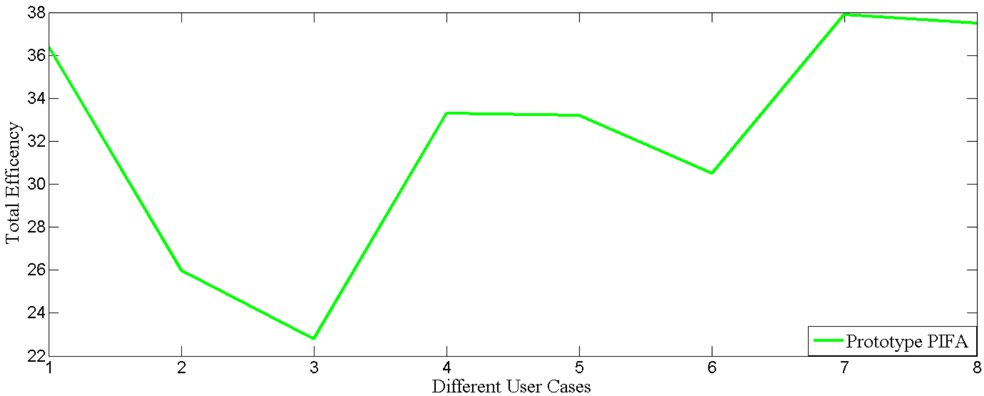


Fig. 43. PIFA Prototype – total efficiency

#### 4.2.1.5 Bezel Prototype

Figure 44 shows the performance of the Bezel Prototype with different DM user cases compared to the performance in free-space. The S parameters behavior of the Bezel Prototype with different user cases shows that the Bezel antenna is more robust against user interaction in the higher band than the lower band due to the Bezel antenna (port 1) having a very wide frequency band in the upper band.

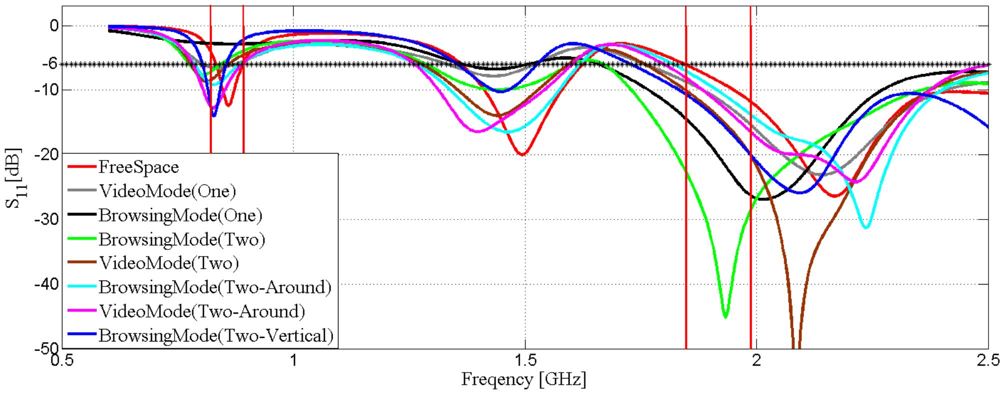


Fig. 44. S parameters of Bezel Prototype with different user scenarios

In the 1HB (One-Hand Browsing Mode) case part of the thumb is very close to the piece of metal that is connected to the feed on port 1. This leads to an obstruction of the radiation pattern of the antenna. In other words, the thumb absorbs a huge amount of the radiated power from the Bezel structure. Furthermore, the close proximity between the thumb and the antenna in 1HB causes a significant reduction in the radiation efficiency at the center frequency in the lower band. The impact of the 2HB (Two-Hand Browsing Mode) case caused a frequency offset in the lower band of 50 MHz. This behavior is due to the location of the fingers around the bezel which changes the current distribution. Moreover, when the thumbs of the two hands are placed in front of the Bezel Prototype, where the main radiation power is focused, the direction of the radiation pattern changes.

Table 5 shows the performance of the Bezel Prototype, from the radiation and total efficiencies point of view, in different user scenarios. The performance of each case depends on the location and the orientation of the user's hand and fingers with respect to the radiating structures on the prototype. Both location and orientation of the hand and fingers cause a change in the characteristic behavior of the antenna through absorption or mismatch. This leads to a radical change in the antenna's radiation and total efficiencies. The worst impact from all user cases is for the cases 2HB and 2HAB. This degradation in the radiation efficiency of these two specific cases is due to the presence of the thumb at the center of the prototype. Since the radiation pattern of the Bezel Prototype is directed from the center of the chassis towards the front of the chassis, the placement of the thumb obstructs the radiation pattern of the Bezel antenna. This leads to a change in the direction of the radiated power.

| User Cases | Radiation Efficiency (%) | Total Efficiency (%) |
|---|---|---|
| Free-space | 85 | 66,5 |
| 1HV | 34.2 | 29 |
| 1HB | 34.5 | 26 |
| 2HB | 20 | 14 |
| 2HV | 32.5 | 26.4 |
| 2HAB | 24 | 19 |
| 2HAV | 36 | 30 |
| 2HVB | 31 | 19 |

Table 5 Total and radiation efficiencies for Bezel Prototype

Figure 45 shows the capacity performance of the Bezel Prototype in different user scenarios. The capacity changes, in a very significant way, according to the change in the correlation value and total efficiency, as shown in Figs. 45 and 46. The capacity of the Bezel Prototype decreases due to the impact of users, especially in the user cases 2HB and 2HAB, as shown in Fig. 45. This is a result of the higher correlation and the lower total efficiency in these cases (see Fig. 46 and 47).

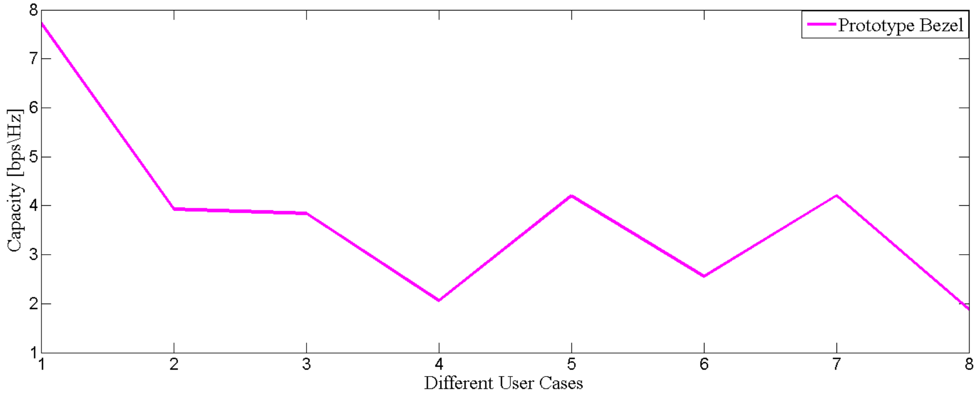


Fig. 45. Bezel Prototype – capacity

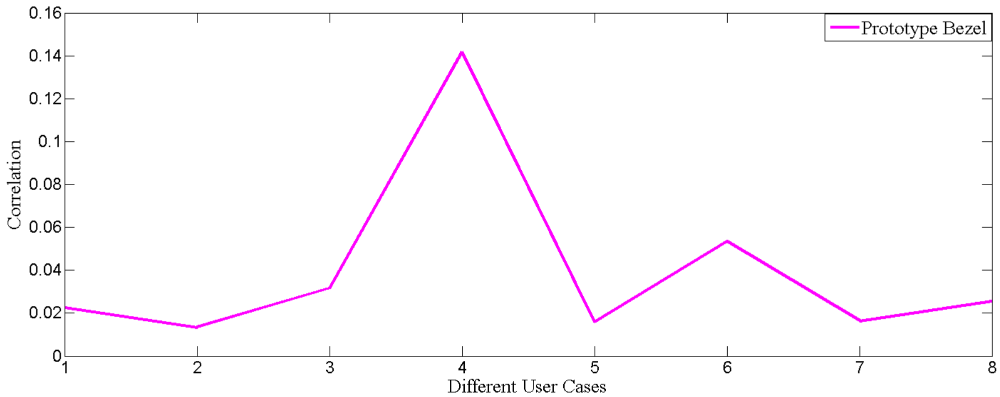


Fig. 46. Bezel Prototype – correlation

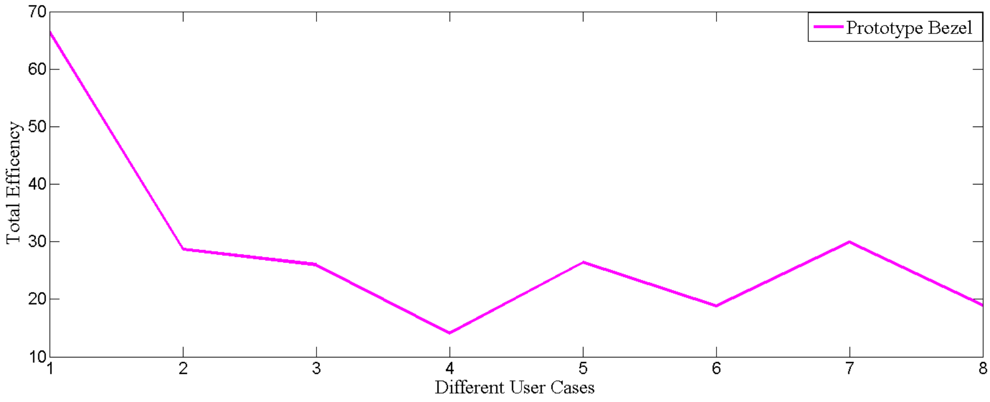


Fig. 47. Bezel Prototype – total efficiency

### 4.2.2 Talk Mode (TM)

As described in Section 3.2.2, all five prototypes have been investigated in three different types of TM scenarios according to the orientation of the terminal with respect to the head. In this section, we focus only on the 60-degree orientation. This case caused the most severe performance degradation due to the proximity to the head and has therefore been chosen for discussion. The remaining results of the different prototypes in the other two orientations are found in the Appendix (Section 7.1).

Figure 48 shows the S parameters for the different prototypes in the 60-degree orientation. The largest impact from user interaction was observed for the Bezel Prototype in the lower frequency band, where the detuning is most severe. Both IFA and PIFA Prototypes have a large frequency offset in the lower frequency band because both prototypes are narrowband. The largest frequency offset of the different prototypes is shown in the IFA Prototype with an 88 MHz offset due to the user interaction. The direction of frequency offset of both the IFA and PIFA Prototypes is different due to the current distribution and radiation patterns of both terminals. In the case of the C-Fed Prototype, the proximity of the antenna elements to the cheek of the head results in high mismatch and absorption losses. Nevertheless, this prototype is wideband and therefore does not suffer as much from the detuning effect of the head.

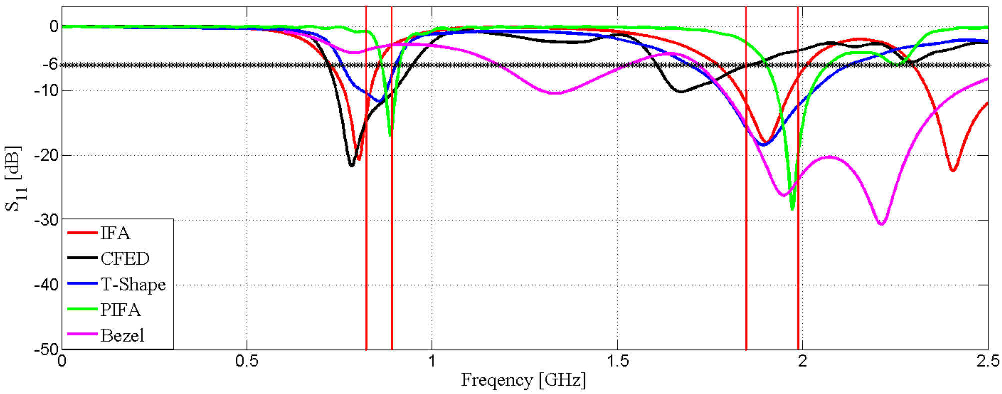


Fig. 48. S parameters for different prototypes in TM (60-degree orientation)

It is noteworthy that the impact of user interaction in TM on all different prototypes (except C-Fed) has smaller effects in the higher frequency band than in the lower frequency band. This is due to higher absorption losses in the lower frequency band as compared to upper band.

## 4.3 Discussion

The impact of user interaction is different for the prototypes depending on the type of antenna used and the setting of each user case. Figure 49 shows the correlation performance of the different prototypes with different DM user scenarios. It is clear how the value of correlation between the antennas in each prototype changes depending on each user setting. All prototypes (except the C-Fed and the Bezel Prototypes) have an increasing correlation value due to the effect of user case 4 (2HB). All three prototypes radiate from the center of the prototype's chassis due to the presence of the thumbs on the sides. In the C-Fed Prototype the location of the elements leads to different user interaction effects. From a correlation point of view, the T-shape and Bezel Prototypes have the least impact from users due to the working principle of these two terminals (reduced correlation by design).

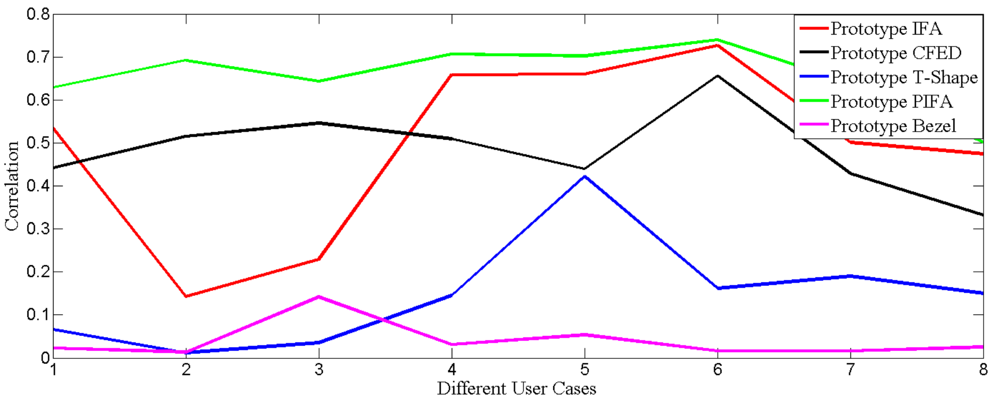


Fig. 49. Correlation for different prototypes with different user scenarios

The capacity performance of different prototypes in different DM user cases is shown in Fig. 50. This figure shows that the T-shape Prototype has the best performance in capacity behavior due to design emphasis on low correlation. The big difference between the T-shape and the Bezel's behavior is the current distribution in both prototypes. The current distribution for the Bezel Prototype is affected by the placement of the hand around the Bezel, whereas in the T-shape case the T-strips are placed on the long edges of the chassis. It is clearly shown that the trend of the capacity for the T-shape, C-Fed, Bezel and PIFA prototypes is roughly the same with different user scenarios. The capacity of these prototypes goes up in user case 2HV, yet goes down in user case 2HAB. The reason behind the difference in behavior for the IFA Prototype is the high coupling between the IFA elements.

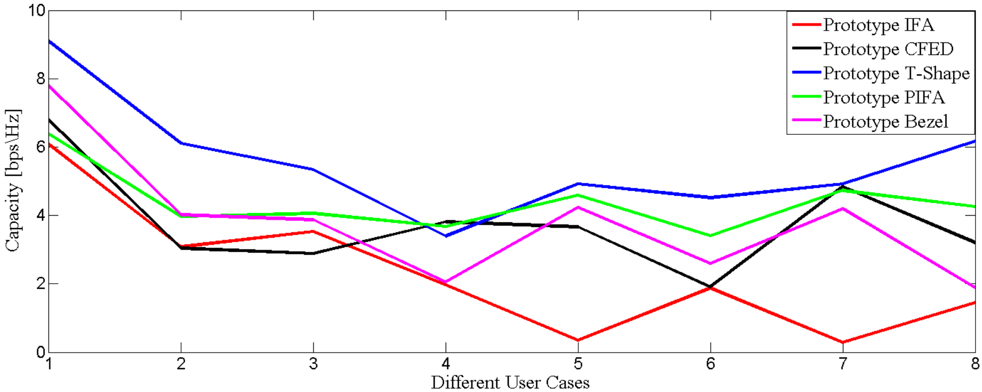

Fig. 50. Capacity for different prototypes with different user scenarios

Table 6 indicates the mean and standard deviation of the frequency offset for each prototype over DM user cases in the lower frequency band. The T-shape Prototype has 8 to 9 times lower value in both mean and standard deviation of the frequency offset as compared to the IFA Prototype. As mentioned earlier, the different directions of the frequency offset of the PIFA resonance frequency with different user scenarios is the reason for the lower value of the mean and the standard deviation for the PIFA Prototype.

Table 7 shows a comparison between the impact of user interaction in TM and the impact of user interaction in DM over all five different prototypes in terms of frequency offset/mismatch efficiency mean and standard deviation. User interactions in TM are more severe than those in

DM from the frequency offset point of view. This is due to the large impact the tissue in the human head has on the radiation power from the antenna. The mean and the standard deviation of the mismatch efficiency for both TM and DM show that the user interaction in both cases has roughly the same effect.

| Antenna Prototypes | Mean [MHz] | Standard deviation [MHz] |
| --- | --- | --- |
| IFA | 95 | 79 |
| C-Fed | 53 | 27 |
| T-Shape | 11 | 10 |
| PIFA | 17 | 13 |
| Bezel | 43 | 8 |

Table 6 Frequency offset for different prototypes

| User Mode | Frequency Offset [MHz] | | Mismatch efficiency | |
| --- | --- | --- | --- | --- |
| | Mean | Standard deviation | Mean | Standard deviation |
| DM | 43 | 36 | 67 | 23 |
| TM | 57 | 37 | 68 | 14 |

Table 7 Frequency offset and mismatch efficiency for TM and DM

# 5 Statistical Modelling

A statistical model gives a description of the probability of a certain event occurring. There are different types of statistical models depending on which probability distribution is used to fit the initial data, such as normal distribution, log normal distribution, Gamma distribution, etc. From an terminal antenna designer's point of view, a statistical model of antennas with realistic user interaction should be beneficial because there is a lot of information that can be extracted and used. It would improve the understanding of the behavior of MIMO antennas without the need to spend effort and time in designing, building and verifying all cases. To find a statistical model implies to formalize the relationship between some given random parameters that vary in different aspects but are related to each other in a stochastic way. Therefore, finding a statistical model that describes different types of antennas with different user interaction scenarios is relevant and has the potential to be extremely beneficial to the terminal antenna community.

Nevertheless, it is not an easy task and includes many different steps and considerations [19]:

1. Examine whether the data comes from a discreet or continuous set.
2. Examine the symmetry of simulated data.
3. Examine if the simulated data has significant trends.
4. Examine if the simulated data has extreme values.

## 5.1 Methods

The way to fit simulated/measured data to one of the known distributions is cumbersome. There are different types of tests/methods that help find the statistical distribution for simulated data like the *Null Hypothesis* method and the *KS-test*. In this project, the *Null Hypothesis* method and the *KS-test* have been used to examine the statistical distribution of the project's simulation data.

The *Null Hypothesis method* is a method used to evaluate the simulated data and examine if it fits with a statistical model depending on a predetermined threshold probability. The *Null Hypothesis* is one of the methods that are used when making decisions for statistical significance. By using this method on simulated data we can know if the data has statistical significance or not. The *Null Hypothesis* method depends on the examination of the simulated data in different cases to find patterns. Then, it tries to find a certain pattern in the simulated data and determines how much this pattern matches the general statistical distribution [20].

To find the exact type of distribution that the simulated data has, the *KS-test* or *Kolmogorov-Smirnov test* is used. The *KS-test* is a method used to return how much the simulated data differs from one of the known distributions.

The different steps to the *KS-test* are:

1. Plot the cumulative distribution function (CDF) or probability distribution function (PDF) of the simulation/measurement data.
2. Plot the CDF/PDF of one of the known distributions.
3. Find the maximum distance between the two CDF/PDF curves ($D_{max}$). See Fig. 51 for more details.
4. Compare the $D_{max}$ found from plotting the data to the theoretical $D_{max}$ that the KS-test provides in the spatial table. Table 8 shows the theoretical table that the KS-test employs.

It is important to mention that choosing which value from the table to use depends on how many points you have in your simulated data and which confidence interval is needed for your purposes [21]. In this project, two frequency bands in five prototypes and 10 user scenarios provide 100 samples for the following statistical analysis.

## 5.2 Results

By applying both methods (*Null hypothesis and KS-test*) to our simulated data, we found very interesting results with a very high degree of accuracy (99% confidence interval). We found that both the radiation and total efficiencies of the MIMO antennas simulated for different prototypes in different user scenarios are statistically significant and each one follows one of the known distributions in both CDF and PDF. In this section, we

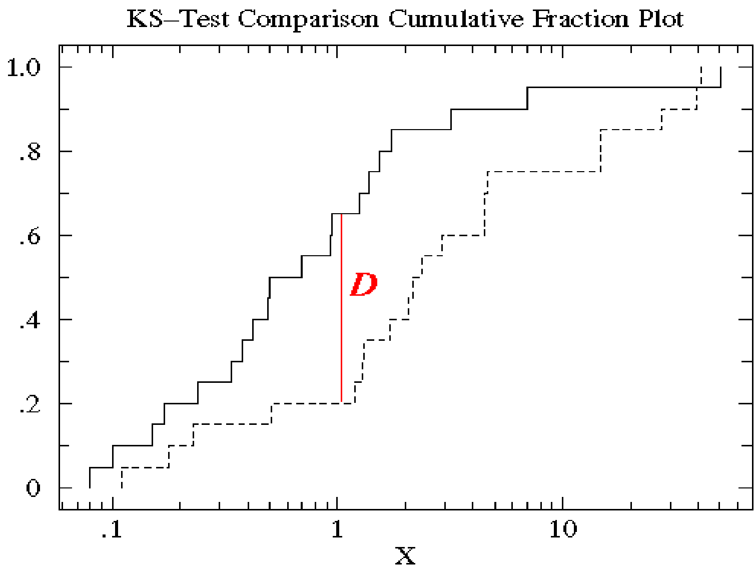


Fig. 51. KS-test

| SAMPLE SIZE (N) | LEVEL OF SIGNIFICANCE FOR D = MAXIMUM [ $F_0(X)$ - $S_n(X)$ ] | | | | |
|---|---|---|---|---|---|
| | .20 | .15 | .10 | .05 | .01 |
| 16 | .258 | .274 | .295 | .328 | .392 |
| 17 | .250 | .266 | .286 | .318 | .381 |
| 18 | .244 | .259 | .278 | .309 | .371 |
| 19 | .237 | .252 | .272 | .301 | .363 |
| 20 | .231 | .246 | .264 | .294 | .356 |
| 25 | .210 | .220 | .240 | .270 | .320 |
| 30 | .190 | .200 | .220 | .240 | .290 |
| 35 | .180 | .190 | .210 | .230 | .270 |
| OVER 35 | $\frac{1.07}{\sqrt{N}}$ | $\frac{1.14}{\sqrt{N}}$ | $\frac{1.22}{\sqrt{N}}$ | $\frac{1.36}{\sqrt{N}}$ | $\frac{1.63}{\sqrt{N}}$ |

Table 8 KS-test table

present the statistical analysis on radiation and total efficiencies for only port 1; however, it has been observed that port 2 provides similar behavior.

The radiation efficiency for port 1 has a lognormal distribution with mean $\mu$ = -0.836 and standard deviation $\sigma$ = 0.415, whereas the total efficiency has a Gamma distribution with the shape parameter of 3.702 and the scale parameter of 0.083. Figure 52 shows the radiation efficiency behavior for all prototypes and user cases tested in a CDF. Figure 53 on the other hand shows the PDF of the radiation efficiency for the five prototypes in the different user scenarios. From the two figures it can be clearly seen that both the CDF and PDF curves for the simulated and the log-normal theoretical data agree very well. The PDF and CDF performance of the total efficiency is shown in Figs. 54 and 55. From these results it is also evident that both the CDF and the PDF performance of the five different prototypes in all user cases match the theoretical Gamma distribution. Therefore, we can conclude that the radiation efficiency and the total efficiency in this study follow known distribution curves with high accuracy and hence the data is applicable as a statistical model.Table 9 shows the statistical behavior of different antenna prototype with different user scenarios from two points of view - mean and standard deviation of both pattern correlation and multiplexing efficiency.

| Prototypes | Correlation | | Multiplexing [dB] | |
|---|---|---|---|---|
| | Mean | Standard deviation | Mean | Standard deviation |
| IFA | 0.391 | 0.239 | -10.874 | 3.813 |
| C-Fed | 0.350 | 0.178 | -8.137 | 2.886 |
| T-Shape | 0.124 | 0.096 | -7.459 | 3.679 |
| PIFA | 0.452 | 0.235 | -8.258 | 2.465 |
| Bezel | 0.039 | 0.025 | -10.305 | 3.140 |

Table 9 Mean and standard deviation for different antenna parameters

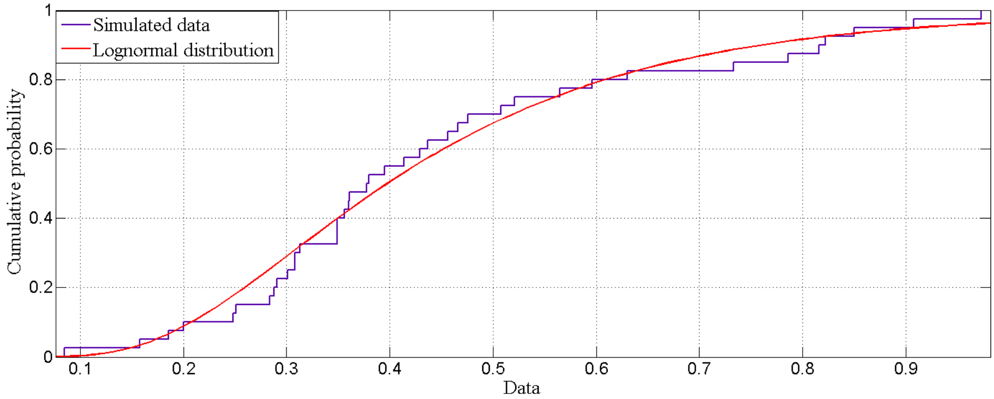


Fig. 52. CDF for radiation efficiency

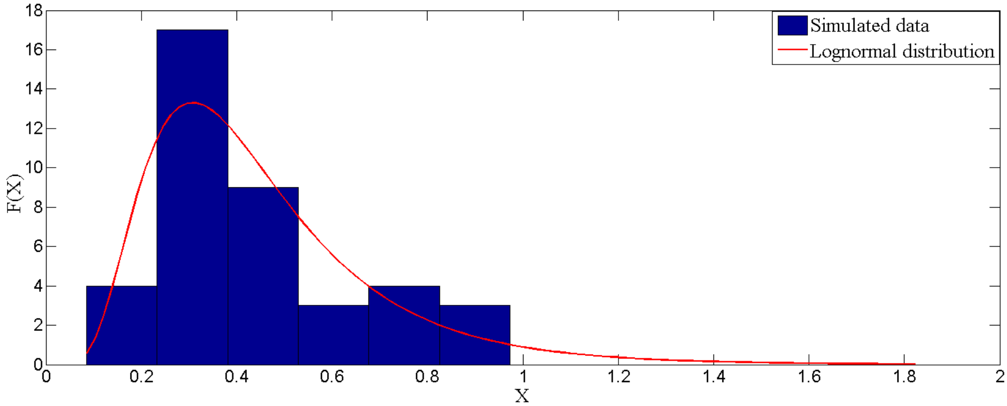


Fig. 53. PDF for radiation efficiency

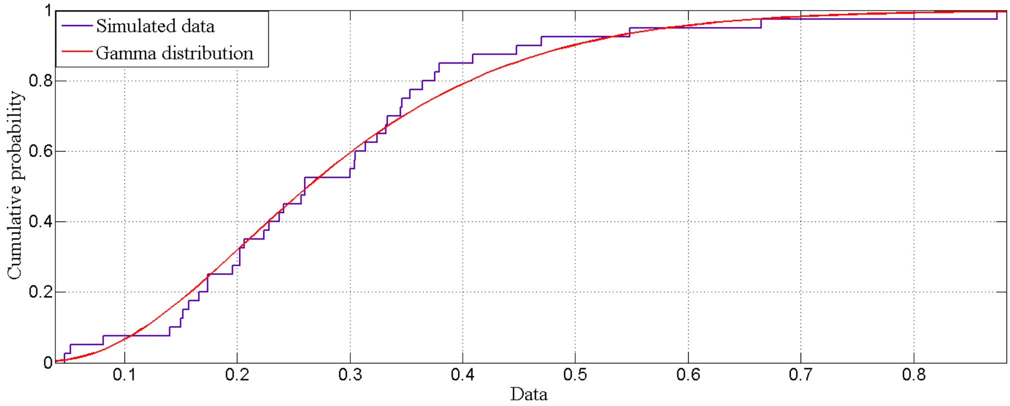


Fig. 54. CDF for total efficiency

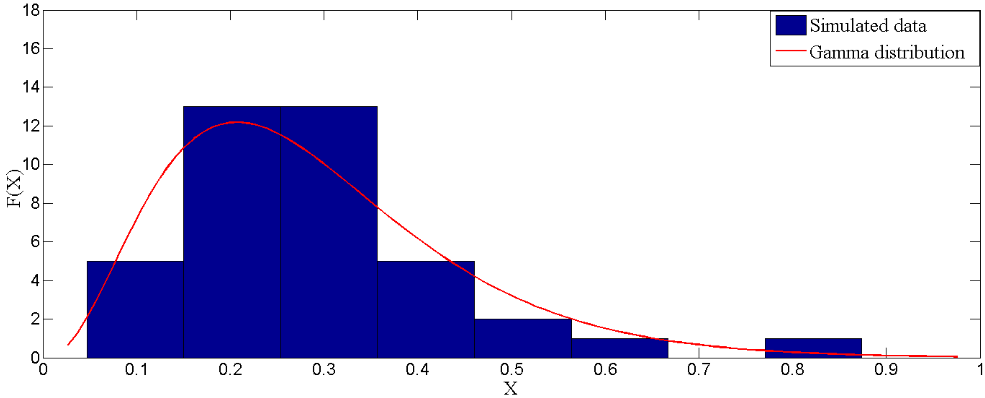


Fig. 55. PDF for total efficiency

# 6 Conclusion and Future Work

In this project, the main goal was reached by building a database with 100 fundamentally different antenna and user cases. The 100 different cases come from the use of five different prototypes with 10 different user scenarios. These are then simulated in two frequency bands, LTE Band 2 and Band 5. A summary of the database is provided in the Appendix (Section 7.2). In the process, we designed and implemented 10 different realistic user scenarios. We were also able to develop a statistical model for both total and radiation efficiencies. The radiation efficiency has a lognormal distribution for the two frequency bands, five prototypes and 10 user cases whereas the total efficiency exhibits a Gamma distribution.

The project results show that user interaction has very significant impact on the behavior of different antenna prototypes. In the cases tested in this study we established that antenna design has a very important role in reducing the impact of user interaction (e.g., IFA vs. T-shape antenna). We also found that the talk mode has a greater impact on different antenna prototypes than the data mode.

There are some aspects of this thesis work that can be extended in future work. For example, instead of only static user scenarios, the statistical study can be performed for dynamic user scenarios, with small movements of the hand grip and the finger positions. In addition, the influence of the propagation channel can be studied by using non-uniform propagation channels. Finally, the project was based entirely on simulation work; measurement verification involving real test persons would be very interesting as future work.

# 7 Appendix

## 7.1 Talk-Mode Results

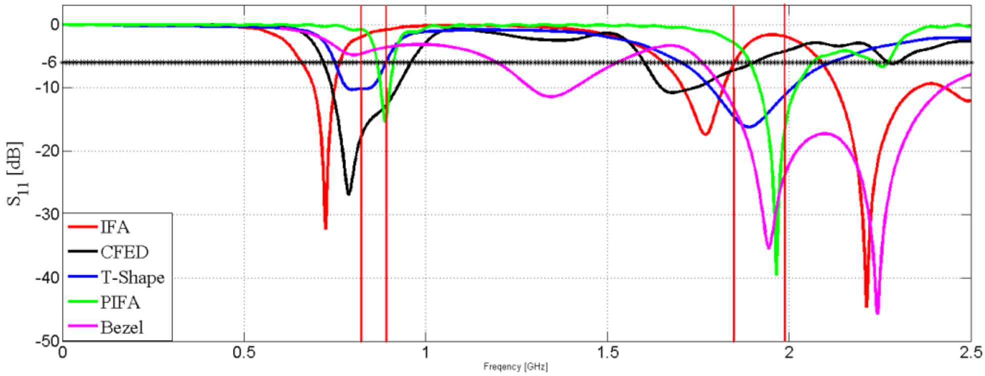


Fig. 56. S parameters for different prototypes in TM (0-degree orientation)

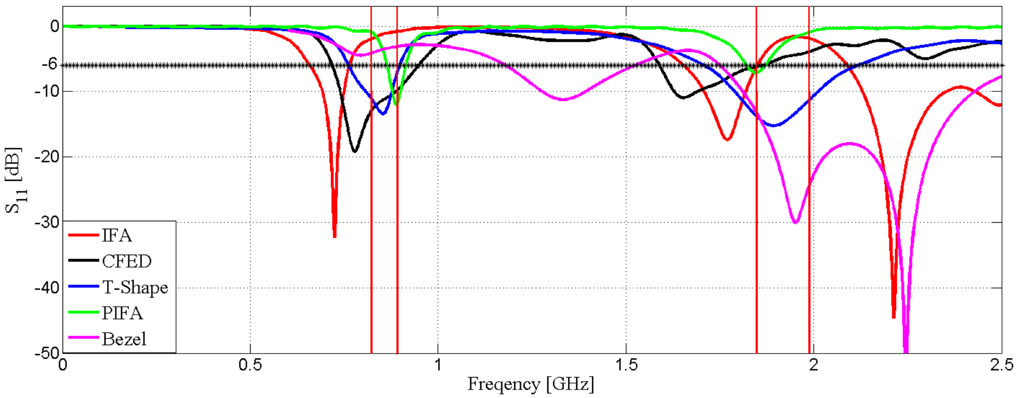


Fig. 57. S parameters for different prototypes in TM (30-degree orientation)

## 7.2 Database

### 7.2.1 Two IFAs (IFA Prototype)

| User Cases | Correlation | | | | | | Multiplexing | | | | | |
|---|---|---|---|---|---|---|---|---|---|---|---|---|
| | Lower | | | Upper | | | Lower | | | Upper | | |
| | 824 | 859 | 894 | 1850 | 1920 | 1990 | 824 | 859 | 894 | 1850 | 1920 | 1990 |
| Free_space | 0,702 | 0,419 | 0,392 | 0,014 | 0,003 | 0,008 | -6,083 | -4,458 | -4,698 | -0,658 | -0,655 | -1,568 |
| One_H_W | 0,17 | 0,563 | 0,395 | 0,02 | 0,034 | 0,006 | -6,153 | -8,078 | -8,958 | -2,931 | -3,785 | -3,667 |
| One _H_B | 0,076 | 0,083 | 0,246 | 0,059 | 0,016 | 0,01 | -5,434 | -6,404 | -8,072 | -3,503 | -2,8965 | -3,292 |
| Two_H_B | 0,58 | 0,58 | 0,615 | 0,044 | 0,027 | 0,009 | -8,365 | -9,874 | -12,035 | -6,673 | -6,701 | -7,198 |
| Two_H_W | 0,63 | 0,625 | 0,612 | 0 | 0,034 | 0,09 | -14,69 | -14,98 | -15,329 | -6,286 | -7,084 | -7,699 |
| Two_H_A_B | 0,608 | 0,701 | 0,74 | 0,003 | 0 | 0,008 | -8,488 | -10,777 | -12,99 | -5,533 | -5,823 | -6,768 |
| Two_H_A_W | 0,618 | 0,549 | 0,485 | 0,052 | 0,015 | 0,003 | -14,17 | -14,971 | -15,614 | -7,911 | -8,24 | -8,735 |
| Two_H_V_B | 0,444 | 0,458 | 0,6 | 0,013 | 0,008 | 0,006 | -6,732 | -7,841 | -9,702 | -4,3 | -3,922 | -4,628 |
| Talk_0_degree | 0,18 | 0,215 | 0,327 | 0,005 | 0,006 | 0,005 | -14,365 | -15,175 | -16,457 | -9,096 | -8,858 | -9,661 |
| Talk_30_degree | 0,061 | 0,105 | 0,201 | 0,002 | 0,002 | 0,001 | -14,501 | -13,582 | -6,082 | -8,992 | -8,529 | -9,11 |
| Talk_60_degree | 0,037 | 0,048 | 0,101 | 0,002 | 0,009 | 0,002 | -12,666 | -13,48 | -15,217 | -8,456 | -7,768 | -8,099 |

### 7.2.2 PIFA-Monopole Antennas (PIFA Prototype)

| User Cases | Correlation | | | | | | Multiplexing | | | | | |
|---|---|---|---|---|---|---|---|---|---|---|---|---|
| | Lower | | | Upper | | | Lower | | | Upper | | |
| | 824 | 859 | 894 | 1850 | 1920 | 1990 | 824 | 859 | 894 | 1850 | 1920 | 1990 |
| Free_space | 0,715 | 0,536 | 0,447 | 0,001 | 0 | 0,005 | -7,817 | -4,679 | -3,856 | -1,896 | -0,46 | -1,558 |
| One_H_W | 0,611 | 0,588 | 0,525 | 0,011 | 0,01 | 0,022 | -9,312 | -7,326 | -7,194 | -4,048 | -4,865 | -6,884 |
| One_H_B | 0,629 | 0,6 | 0,535 | 0,01 | 0,009 | 0,02 | -10,012 | -7,356 | -6,553 | -3,869 | -2,994 | -4,734 |
| Two_H_B | 0,696 | 0,628 | 0,603 | 0,004 | 0,003 | 0,006 | -8,457 | -7,933 | -9,447 | -7,511 | -6,444 | -7,252 |
| Two_H_W | 0,77 | 0,684 | 0,658 | 0,045 | 0,051 | 0,039 | -8,954 | -7,2 | -7,543 | -6,371 | -5,268 | -5,433 |
| Two_H_A_B | 0,683 | 0,642 | 0,593 | 0,027 | 0,014 | 0,011 | -9,063 | -8,314 | -8,889 | -6,223 | -5,793 | -7,21 |
| Two_H_A_W | 0,644 | 0,549 | 0,529 | 0,005 | 0,008 | 0,009 | -7,316 | -6,323 | -7,228 | -6,599 | -5,678 | -6,267 |
| Two_H_V_B | 0,513 | 0,446 | 0,385 | 0,001 | 0 | 0 | -8,304 | -6,322 | -6,544 | -4,254 | -4,026 | -5,813 |
| Talk_0_degree | 0,308 | 0,131 | 0,127 | 0,011 | 0,006 | 0,009 | -14,982 | -11,949 | -10,96 | -11,744 | -9,42 | -9,907 |
| Talk_30_degree | 0,157 | 0,108 | 0,104 | 0,022 | 0,021 | 0,022 | -14,776 | -11,76 | -10,65 | -11,104 | -8,746 | -9,14 |
| Talk_60_degree | 0,1 | 0,06 | 0,05 | 0,021 | 0,018 | 0,019 | -14,583 | -11,679 | -10,23 | -10,969 | -8,606 | -8,993 |

### 7.2.3 Two C-Fed Antennas (C-Fed Prototype)

| User Cases | Correlation | | | | | | Multiplexing | | | | | |
|---|---|---|---|---|---|---|---|---|---|---|---|---|
| | Lower | | | Upper | | | Lower | | | Upper | | |
| | 824 | 859 | 894 | 1850 | 1920 | 1990 | 824 | 859 | 894 | 1850 | 1920 | 1990 |
| Free_space | 0,347 | 0,43 | 0,499 | 0,008 | 0,014 | 0,009 | -3,587 | -3,834 | -4,169 | -1,031 | -1,042 | -1,408 |
| One_H_W | 0,435 | 0,525 | 0,562 | 0,051 | 0,034 | 0,018 | -7,971 | -8,069 | -7,937 | -3,741 | -3,785 | -4,097 |
| One_H_B | 0,435 | 0,507 | 0,53 | 0,161 | 0,015 | 0,126 | -8,178 | -8,206 | -8,08 | -5,133 | -5,339 | -5,772 |
| Two_H_B | 0,449 | 0,448 | 0,461 | 0,007 | 0,014 | 0,013 | -6,557 | -6,847 | -7,132 | -5,81 | -6,019 | -6,654 |
| Two_H_W | 0,556 | 0,567 | 0,598 | 0,009 | 0 | 0 | -7,312 | -7,561 | -7,91 | -5,011 | -5,094 | -5,657 |
| Two_H_A_B | 0,392 | 0,362 | 0,352 | 0,023 | 0,033 | 0,04 | -5,779 | -5,812 | -5,978 | -5,207 | -5,51 | -6,166 |
| Two_H_A_W | 0,402 | 0,407 | 0,427 | 0,031 | 0,044 | 0,05 | -5,462 | -5,571 | -5,804 | -6,102 | -6,232 | -6,964 |
| Two_H_V_B | 0,248 | 0,322 | 0,336 | 0,001 | 0,002 | 0,006 | -6,556 | -7,077 | -7,424 | -6,562 | -6,535 | -6,527 |
| Talk_0_degree | 0,026 | 0,045 | 0,091 | 0,016 | 0,015 | 0,025 | -11,092 | -11,497 | -11,841 | -11,277 | -11,665 | -12,667 |
| Talk_30_degree | 0,09 | 0,136 | 0,189 | 0,051 | 0,105 | 0,179 | -11,974 | -12,528 | -12,988 | -12,579 | -13,133 | -14,23 |
| Talk_60_degree | 0,09 | 0,111 | 0,168 | 0,055 | 0,098 | 0,166 | -12,001 | -12,506 | -13,008 | -12,1 | -12,59 | -13,77 |

## 7.2.4 T-Shape-Monopole Antennas (T-Shape Prototype)

| User Cases | Correlation | | | | | | Multiplexing | | | | | |
|---|---|---|---|---|---|---|---|---|---|---|---|---|
| | Lower | | | Upper | | | Lower | | | Upper | | |
| | 824 | 859 | 894 | 1850 | 1920 | 1990 | 824 | 859 | 894 | 1850 | 1920 | 1990 |
| Free_space | 0,14 | 0,071 | 0,048 | 0,017 | 0,08 | 0,038 | -3,805 | -2,301 | -2,538 | -1,906 | -1,716 | -1,963 |
| One _H_W | 0,074 | 0,022 | 0,169 | 0,127 | 0,07 | 0,002 | -4,945 | -5,103 | -3,442 | -3,233 | -3,233 | -3,65 |
| One_H_B | 0,133 | 0,03 | 0,149 | 0,137 | 0,136 | 0,005 | -5,921 | -4,952 | -5,508 | -4,82 | -4,7 | -5,143 |
| Two_H_B | 0,105 | 0,126 | 0,069 | 0,063 | 0,016 | 0,01 | -6,791 | -7,166 | -7,427 | -6,854 | -6,858 | -7,273 |
| Two_H_W | 0,285 | 0,378 | 0,359 | 0,114 | 0,161 | 0,046 | -6,439 | -6,282 | -6,56 | -5,76 | -5,878 | -6,07 |
| Two_H_A_B | 0,113 | 0,117 | 0,083 | 0,052 | 0,071 | 0,038 | -6,199 | -6,199 | -6,433 | -6,327 | -6,391 | -6,743 |
| Two_H_A_W | 0,201 | 0,171 | 0,092 | 0,164 | 0,121 | 0,017 | -6,047 | -5,971 | -6,465 | -6,431 | -6,305 | -6,405 |
| Two_H_V_B | 0,015 | 0,162 | 0,078 | 0,185 | 0,031 | 0,015 | -6,412 | -5,5 | -5,42 | -5,518 | -5,11 | -5,545 |
| Talk_0_degree | 0,196 | 0,106 | 0,038 | 0,134 | 0,053 | 0,009 | -12,475 | -12,658 | -13,679 | -10,119 | -9,972 | -10,212 |
| Talk_30_degree | 0,142 | 0,111 | 0,056 | 0,131 | 0,06 | 0,007 | -12,741 | -13,265 | -14,926 | -10,154 | -9,851 | -9,83 |
| Talk_60_degree | 0,104 | 0,08 | 0,093 | 0,107 | 0,037 | 0,011 | -12,428 | -12,662 | -13,73 | -9,44 | -9,248 | -9,459 |

### 7.2.5 Bezel Prototype

| User Cases | Correlation | | | | | | Multiplexing | | | | | |
|---|---|---|---|---|---|---|---|---|---|---|---|---|
| | Lower | | | Upper | | | Lower | | | Upper | | |
| | 824 | 859 | 894 | 1850 | 1920 | 1990 | 824 | 859 | 894 | 1850 | 1920 | 1990 |
| Free_space | 0,005 | 0,029 | 0,058 | 0,044 | 0,005 | 0,035 | -6,269 | -5,333 | -5,954 | -4,077 | -4,083 | -4,213 |
| One_H_W | 0,112 | 0,101 | 0,101 | 0,067 | 0,028 | 0,037 | -7,766 | -8,827 | -10,08 | -5,219 | -5,403 | -5,83 |
| One_H_B | 0,014 | 0,012 | 0,013 | 0,033 | 0 | 0,051 | -12,909 | -13,73 | -12,601 | -7,595 | -7,714 | -7,717 |
| Two_H_B | 0,02 | 0,033 | 0,042 | 0,144 | 0,098 | 0,062 | -9,662 | -9,689 | -9,754 | -9177 | -9,432 | -9,713 |
| Two_H_W | 0,035 | 0,059 | 0,079 | 0,032 | 0,013 | 0,008 | -8,014 | -8,607 | -8,979 | -7,768 | -8,011 | -8,435 |
| Two_H_A_B | 0,009 | 0,016 | 0,023 | 0,261 | 0,141 | 0,046 | -8,556 | -8,662 | -8,794 | -8,846 | -8,821 | -8,84 |
| Two_H_A_W | 0,01 | 0,022 | 0,034 | 0,271 | 0,196 | 0,114 | -6,92 | -7,235 | -7,539 | -8,226 | -8,338 | -8,484 |
| Two_H_V_B | 0,008 | 0,039 | 0,074 | 0,068 | 0,03 | 0,098 | -9,427 | -10,489 | -10,927 | -7,163 | -7,151 | -7,293 |
| Talk_0_degree | 0,074 | 0,056 | 0,039 | 0,151 | 0,075 | 0,01 | -13,472 | -13,413 | -13,442 | -9,971 | -10,431 | -10,998 |
| Talk_30_degree | 0,039 | 0,027 | 0,017 | 0,066 | 0,027 | 0,001 | -11,113 | -11,233 | -11,509 | -10,314 | -10,802 | -11,316 |
| Talk_60_degree | 0,053 | 0,039 | 0,03 | 0,075 | 0,043 | 0,009 | -16,907 | -16,138 | -15,837 | -10,407 | -10,642 | -10,99 |

# 8 References


[1] http://niviuk.free.fr/lte_band.php [Online].

[2] http://www.cst.com [Online].

[3] A. Paulraj, R. Nabar, D. Gore, *Introduction to Space-Time Wireless Communication*, Cambrige University Press, 2008.

[4] A. M. Tulino, A. Lozano, and S. Verdú, "Impact of antenna correlation on the capacity of multiantenna channels," *IEEE Trans. Inform. Theory*, vol. 51, no. 7, pp. 2491-2508, Jul. 2005.

[5] http://www.antenna-theory.com [Online].

[6] C. A. Balanis, *Antenna Theory: Analysis and Design*, 3rd edition, Wiley, July 2009.

[7] http://www.antenna-theory.com/antennas/main.php. [Online].

[8] R. Whiton and F. Firouzabadi, "Co-located antenna design in a mobile phone," *MSc Thesis*, Dept. EIT, Lund University, Jun. 2012.

[9] H. Li, Z. Miers, and B. K. Lau, "Design of orthognal MIMO handset antennas based on characteristic mode manipulation at frequency bands below 1GHz," *IEEE Trans. Antennas Propag.*, to appear.

[10] Z Miers, H. Li, and B. K. Lau, "Design of bezel antennas for multiband MIMO terminals using characteristic modes," in *Proc. 8th Europ. Conf. Antennas Propag. (EuCAP'2014)*, The Hague, The Netherlands, Apr. 6-10, 2014.

[11] V. Plicanic Samuelsson, B. K. Lau, A. Derneryd, and Z. Ying, "Channel capacity performance of multi-band dual antenna in proximity of a user," in *Proc. Int. Workshop Antenna Technol. (IWAT '2009)*, Santa Monica, LA, Mar. 2-4, 2009.

[12] R. Tian, B. K. Lau, and Z. Ying,, ""Multiplexing efficiency of MIMO antennas," *IEEE Antennas Wireless Propag. Lett.*, vol. 10, pp. 183-186, 2011.

[13] V. Plicanic, I. Vasilev, R. Tian, and B. K. Lau, "Capacity maximisation of handheld MIMO terminal with adaptive matching in indoor environment,"

*Electron. Lett.*, vol. 47, no. 16, pp. 900-901, Aug. 4, 2011..

[14] V. Plicanic, B. K. Lau, A. Derneryd, and Z. Ying, "Actual diversity performance of a multiband antenna with hand and head effects," *IEEE Trans. Antennas Propag*., vol. 57, no. 5, pp. 1547-1556, May 2009.

[15] A. Sibille, "Statistical modeling of the radio-electric properties of wireless Terminals in their environment," *IEEE Antennas Propag. Mag*. vol. 54, no. 6, pp. 117-129, Dec. 2012.

[16] M. Pelosi, O. Franek, M. B. Knudsen, M. Christensen, and G. F. Pedersen, "A grip study for talk and data modes in mobile phones," *IEEE Trans. Antennas Propag*., vol. 57, no. 4, pp. 856-865, Apr. 2009.

[17] A. A. H. Azremi, V. Papamichael , and P. Vainikainen, "Multi-antenna mobile terminal diversity performance in proximity to human hands under different propagation environment conditions," *IET Electron. Lett*., vol. 47, no. 22, pp. 1214-1215, Oct. 27, 2011.

[18] R. Hosseinzadeh and B. Zakeri, "SAR of the human head due to electromagnetic radiation of a mobile antenna," in P*roc. 20th Telecommunications Forum (TELFOR)*, Belgrade, Serbia, Nov 20-22, 2012, pp. 1159-1161.

[19] http://pages.stern.nyu.edu/~%20adamodar/New_Home_Page/StatFile/stat distns.htm. [Online].

[20] http://en.wikipedia.org/wiki/Null_hypothesis. [Online].

[21] http://www.physics.csbsju.edu/stats/KS-test.html. [Online].

[22] J. Ilvonen, O. Kivekäs, J. Holopainen, R. Valkonen, K. Rasilainen, and P. Vainikainen, "Mobile terminal antenna performance with the user's hand: effect of antenna dimensioning and location," *IEEE Antennas Wirelss Propag. Lett*., vol. 10, pp. 772-775, 2011..

[23] B. K. Lau, J. B. Andersen, G. Kristensson and A. F. Molisch, "Antenna matching for capacity maximization in compact MIMO systems," in *Proc. 3rd Int. Symp. Wireless Commun. Syst. (ISWCS'2006)*, Valencia, Spain, Sep. 5-8, 2006, pp. 253-257.

LUND UNIVERSITY

http://www.eit.lth.se